Advanced Materials Research *Online: 2010-10-19*
ISSN: 1662-8985, Vol. 137, pp 81-128
doi:10.4028/www.scientific.net/AMR.137.81

Production of customized high-strength hybrid sandwich structures

Olga Sokolova[1,a], Adele Carradó[2,b], Heinz Palkowski[1,c]

[1]Institute of Metallurgy (IMET), Metal Forming and Processing,
Clausthal University of Technology (TUC),
Robert-Koch-Str. 42, 38678 Clausthal-Zellerfeld, Germany

[2]Institut de Physique et Chimie des Matériaux de Strasbourg, IPCMS, UMR 7504 ULP-CNRS,
23 rue du Lœss, BP 43, 67034 Strasbourg cedex 2, France

[a]olga.sokolova@tu-clausthal.de, [b]werkstoffumformung@tu-clausthal.de
[c]heinz.palkowski@tu-clausthal.de

Keywords: sandwich composite, reinforcement, formability, bonding, deep drawing, bending, local properties

Abbreviations

CC:	carbon- carbon
CH:	carbon-hydrogen
CT:	corona treatment
DIC:	digital image correlation
ER:	elongation to rupture
F_{BH}:	blank-holder force
FEM:	finite element method
FLC:	forming limit curve
FLD:	forming limit diagram
GLARE:	GLAss-REinforced
PE:	polyethylene
PP:	polypropylene
PP-PE:	polyolefin
RB:	roll-bonding process
RD:	rolling direction
RE:	reinforcing elements
SD:	standard deviation
SMS:	sandwich composite materials
TS:	tensile strength
YS:	yield strength

Abstract. The production process and the forming behaviour of locally reinforced steel/polymer/steel (316L/PP-PE/316L) hybrid sandwich composite materials (SMS) have been investigated. The effect of simple plate reinforcements with different size, shape and geometry on the forming limits of SMS was studied. As a local reinforcement, the simple solid steel and mesh steel plate inlays with central and edge positions were chosen instead of a polymer core as a sandwich laminate. In order to increase the adhesion properties between the metal and polymer layers, corona discharge and plasma preliminary surface treatments were applied prior to the sandwich production.

Both, deep drawing and stretching cup-forming tests were performed in order to analyse the forming behaviour as well as the failure of SMS with and without local inlays subject to different tensile loadings. The influence of the local reinforcement on the bending behaviour was determined by three and four-point bending processes. Stress-strain curves and thinning behaviour of SMS with local reinforcements under the different forming loads were determined using digital image correlation via photogrammetry.

The forming behaviour strongly depends on the quality, geometry and size of the local plate inlays. Owing to the different positions of reinforcement as well as to the different polymer content around of inlays, failure of SMS by bending and drawing differs. The sandwich samples with mesh reinforcement demonstrate better formability by drawing and bending than that of samples with solid plates. In order to minimise the loss in formability of sandwich samples during deep drawing, the size of the centred reinforcement has to be larger than the punch diameter.

Introduction

Owing to their optimally adaptable design structures, sandwich composite materials [1] - here in particular three layered metal-polymer-metal sheets, abbreviated as SMS in the following - can have excellent properties [2,3] They find their applications in the automotive [4], shipbuilding and aerospace industries [5]. Due to the metal cover sheets, bonded together with a soft thermoplastic polymer core, metal-polymer based sandwich composite materials represent a good combination of high stiffness and strength, as well as good deep drawing and forming properties under different conditions. Using adequate cover materials even their corrosion resistance is fitting well [6]. Moreover they show good dynamic and static loading, and high damping [7] and acoustic properties due to the polymer core.

Research activities are increasing in order to develop SMS with a high potential for forming and design as well as lightweight constructions and low production costs. Depending on the material used and the design of the parts, various methods are in use for sandwich laminate production**,** surface treatments for increasing the adhesion between the sandwich's components and forming processes of these laminates.

Currently, many industrial scientific projects and research groups are working in the fields of manufacturing, bonding, forming, reinforcements, mechanical and thermal joining of SMS. They show special interest in exploring areas for composites' design and their applications. As a result, sandwich constructions have been used in many fields of industry. For example, Bondal [8], developed by ThyssenKrupp Steel AG, is based on two covering steel sheets bonded with a polymer core in the range of some ten microns. This SMS is aimed at high damping capacity, high formability and corrosive resistance and is well established in the automotive industry. Another example is the famous high-tech GLARE [9, 10] sandwich composite being used in the Airbus A 380. Indeed, twenty seven skin panels of the fuselage are made of GLARE resulting in a strong weight saving compared to the conventional aluminium panels. This sandwich consists of multi-layered glass fibre reinforced aluminium. The aluminium sheets have thicknesses of 0.2 mm to 0.5mm and the glass ply has a thickness of 0.125 mm.

One representative of a 3-layered sandwich composite laminate is the Hylite composite, which consists of aluminium-polypropylene-aluminium sheets with a thickness of 0.2/0.8/0.2 mm [11]. Due to the plastic core and metallic cover sheets, good corrosion resistance, sound and damping properties, good formability by deep drawing, stretching and shear cutting, punching and forming can be observed in Hylite. It has already been introduced into several profitable applications, e.g. in the automotive market, been used for top floor panels and new roof designs in concept cars. As a material for the aircraft and shipbuilding industries, Hylite provides low weight and high rigidity being important for these applications [10].

Processing. Today, one of the commonly used methods for the continuous and discontinuous production of metal-polymer metal sandwich materials is the roll-bonding (RB) process [12-14], which can be realized with and without glue adhesive agents. This process has been widely used in the laboratory production of metal-polymer based sandwich laminates. For bonding the metal to the polymer sheets, an adhesive, e.g. epoxy resin, has to be used for laboratory RB manufacturing [15-17]. During the manufacturing of metal-polymer sandwich materials, the same methods for roll-bonding can be used to increase the adhesion between the layers. For example, in [18] an alternative method of adhesively bonded joints for metal-polymer composites have been investigated, such as surface treatments, adhesive materials systems and methods of analysing the bonding quality as

well as mechanical and thermal surface pre-treatments. So, corona and plasma treatments can improve the bonding between the sandwich layers by increasing the adhesion between the metal/polymer layers. These treatments are effective methods in discontinuous and continuous sandwich production processes.

Surface treatment methods. Corona treatment functions by raising the polymer's surface energy and improving the adhesive characteristics through creating multiple bonding sites [19]. Corona is an atmospheric plasma treatment, by which a gas is ionized by applying a high potential between two electrodes thus creating a discharge.

Plasma surface treatment offers innovative solutions to adhesion and wetting problems in many industries. The purpose of plasma surface treatment of polymer- and metal-based materials is to increase surface wettability by attacking the material surface via electrical discharge. Surface treatment with plasma results in good wetting of the material surface and thereby improving the surface adhesion properties [20].

Corona treatment is a common method for increasing surface energy and adhesion, for activating and cleaning substrates (metals and polymers), prior to the production, and products after manufacturing [21]. The treatment improves the interaction of the surface with adhesives (e.g. epoxy resin) as well as the wettability of the surface [22]. Noeli [23], Pascual [24] and Zhang [22] have shown that the presence of polar groups and the morphology of the polyolefin film's surface play a very important role for obtaining good adhesion. Polypropylene films have limitations to their adhesion properties due to both their non-polar nature and low surface tension. In contrast to the hot plasma method, the corona treatment can be used very precisely because of its low discharge temperature. Polyolefin foil (e.g. PP-PE, *been used as core material for our SMS*) contains long molecular chains that form a strong and uniform product. The attachment of the corona onto the polymer can be described as an anchoring of atoms or air molecules onto the polymer surface. The corona is used to introduce reactive groups onto the poor, non-polar polymer surface. A portion of the radicals are stabilized on the polymer surface after exposure to the corona-treatment's discharge (see Fig.1).

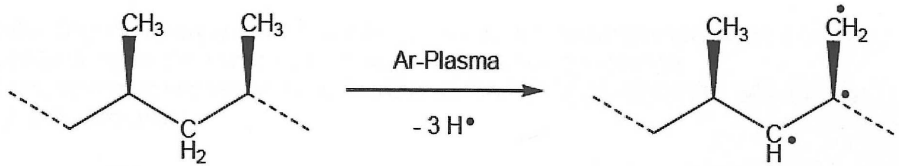

Fig. 1. Schematic representation of free radical formation by corona treatment according to [23]

These radicals react with atmospheric oxygen in order to form hydrophilic groups, which can increase the surface wettability. It can react such that, e.g. corona with oxygen (air as a probable source), hydroxyl and carboxyl groups in the polyolefin surfaces are introduced by increasing the hydrophilicity of the surface, and the improved wettability of the surface is disrupted (see Fig. 2).

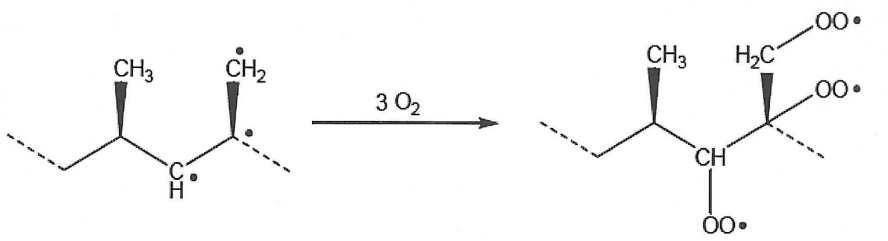

Fig. 2. Schematic representation of the reaction of oxygen with the corona formed macro-radicals

The peroxygen reacts with hydro-peroxide and finally forms hydroxyl-carbonyl or carbonyl groups (Fig. 3).

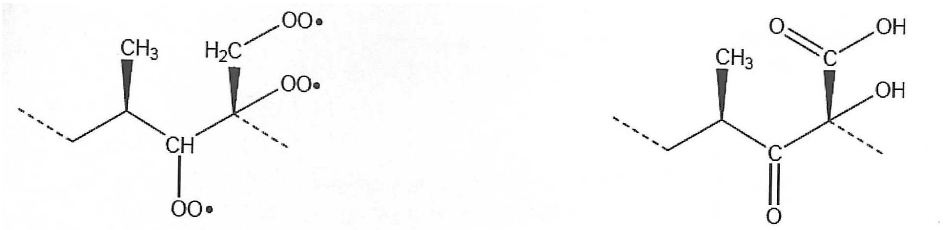

Fig. 3. Schematic representation of the formation of hydroxyl, carbonyl and carboxyl groups

As a result, the corona effect on the polymer surface can be schematically depicted as (see Fig. 4):

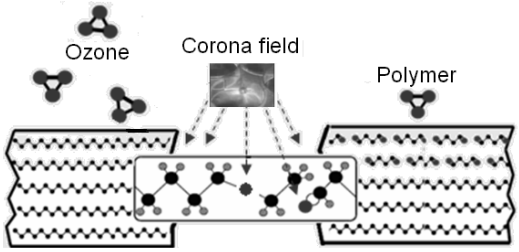

Fig. 4. Set-up of the corona discharge for the polyolefin foil

This process concentrates on the polymer surface at normal ambient atmospheric pressure and high-voltage electric field. The electrons of the electric field are highly accelerated, such as the oxygen or nitrogen oxides. Here, as the process of ionization of the free electrons progresses new molecules are formed on the polymer surface. These exist at the contact surface with the energy of CC or CH bonds. The following reactions were observed: degradation of the macromolecules' reaction, networking reactions and the formation of so called "free macro radicals" [23].

Mechanical and forming studies. A wide range of investigations of the forming behaviour corresponding to industrial applications of SMS such as vehicle body parts, e.g. bending or deep drawing tests, are finding a special place in the future of sandwich composite development. This is useful in the production of vehicle roofs, bonnets and other parts of vehicle's body. Many investigations [25-30] show good formability properties e.g. by deep drawing metal-polypropylene-metal SMS, based on aluminium or steel, cover sheets and plastic core layers at room temperature in comparison to the simple mono-materials.

To define the field of application for SMS the observation and characterisation of the forming behaviour as well as the determination of the Forming Limit Curves (FLC) by stretching and deep drawing test using Nakashima samples is suitable. FLCs are very useful for analyzing the actual and potential problems in sheet forming. They are often considered to be the actual curve in the forming limit diagram (FLD). The FLD indicates the major strain to failure as a function of the minor strain for different paths of load. The FLC is a convenient representation of the material's ultimate ductility influenced by various strain conditions and given boundary criteria such as failure or the onset of necking. They are also used as a parameter in finite element analysis either to determine where the material exceeds the level of formability or to compare the formability of different materials. The influence of temperature on the forming behaviour (FLD) of aluminium/polypropylene/aluminium composites in deep drawing was investigated in [26]. This work shows a significant change in the viscoelastic - plastic level of the core, thereby decreasing the drawability by increasing the forming temperature and reducing the spring-back effect in drawing tests.

In the work of Weiss et al. [27] the influence of polymer interlayer thickness and strength on steel-polymer-steel sandwich composite behaviour was investigated by means of the bending

process. The sandwiches process by hot laminating showed that the spring-back effect by bending was significantly decreased by increasing the polypropylene or polyvinyl chloride interlayer thickness and decreasing of strength of interlayer material. Other investigations [31-33] analysed the spring-back effect on the mechanical properties of metal-polymer-SMS by using different bending conditions.

Finite Element Method simulation. The behaviour of the sandwich composite at different degrees of bending was observed and analysed and modelled using finite element method (FEM). The study of damping, vibration and acoustic properties of polymer-core based laminates is currently being strongly under development. An evaluation of the damping of sandwich materials fabricated with different polymer cores and laminated steel or aluminium skins was presented in [34, 35].

The mechanical characterisation is based on the theory of sandwich plates and a FEM analysis of the vibrations in a sandwich composite body [36]. Good damping subject to bending, torsion and vibration tests could be observed due to the soft core. This also was proven by FEM simulation for complex sandwich parts. Different modelling and simulation procedures were applied to the sandwich plates. The most important processes studied were deep drawing, bending processes and crash behaviour [37]. These articles present an analysis of stress-strain properties, the changes in the structure and other important factors as the forming behaviour of the sandwich material and also the behaviour of sandwich components in the construction subject to complex loading.

Reinforced sandwiches. Local reinforcement in metal-polymer-metal sandwich composites is a necessity, if these parts are to be connected with other ones by mechanical (bolting) or thermal (welding) joining. Without reinforcement the system might loose its pre-stressing force over time in the first case, in case of thermal load the polymer can be vaporized and cause corrosion. Due to the different materials (solid steel, mesh steel), geometry, size and local position of the inlays, the forming behaviour of these structures can differ strongly. Additionally the sensitivity to wrinkling during deep drawing is stronger than for the mono steel materials because of the soft core of the sandwich [38].

A sufficiently large and separate area is devoted to the study of mechanical and thermal joints of sandwich materials in the construction. Mechanical fastenings, such as various screw and bolt joining methods [39, 40] as well as specially designed inserts and adaptors [41] were investigated according to [42, 43]. On the other hand, analysis of laser and thermal welding also had been done in several investigations on sandwich composites; however, in this case the local plate reinforcement or special adaptors, in place of welding, have to be used instead of the polymer layer. In both cases, special local plate inserts in the core layer, or across all layers, will be used for sandwich systems like a key to mechanically and thermally join metal-polymer sandwich based composites for important industrial devices and constructions.

The main and important question of increasing the adhesion between the polymer and metal layers as well as the status of mechanically and thermally joining metal-polymer systems according to their direct applications, e.g. in the automotive industry, have not been sufficiently studied. The project A3 deals with this topic, the production, manufacturing and the subsequent treatment of partially strengthened three layered, symmetrical sandwich structures. Fig. 5 gives an overview of the main steps and investigations within this project. In order to obtain a basic understanding and – probably - improved applications of sandwich laminates for automotive and aircraft applications, the formability behaviour of metal-polymer-metal sandwich laminates was investigated with and without different, simple local plate reinforcement subject to different and complex forming processes.

The main aims of this – still running - research are:

- Developing a method for manufacturing local reinforced SMS,
- Investigating the mechanical properties of sandwich composites without and with locally reinforcement,
- Correlating the various simple shape, size and material of reinforcement with the formability of SMS, and
- Analyse the fields of applications for reinforced SMS based on the formability data.

The sandwich composite acquires the ability to fulfil certain tasks due to the local reinforcement as follow:

- The behaviour of the sandwich composite under simple and complex loading could be significantly improved due to the local strengthening in the reinforced region,
- Mechanical or thermal joining should be possible at the reinforced region, owing to this phenomenon the problem of the polymer core layer melting in the weld-seam can be avoided during the welding process. This problem may lead to pore formation or failure of the sandwich specimen,
- Some functions may be integrated into the core layer, such as a sensor, to act as an active element, e.g. for a crash controller or to assume controlling functions such as relevant strain changes.

Due to the different inlay-materials, their quality, geometry and size as well as the position of local inlays, the forming behaviour of sandwich reinforced structures can differ significantly.

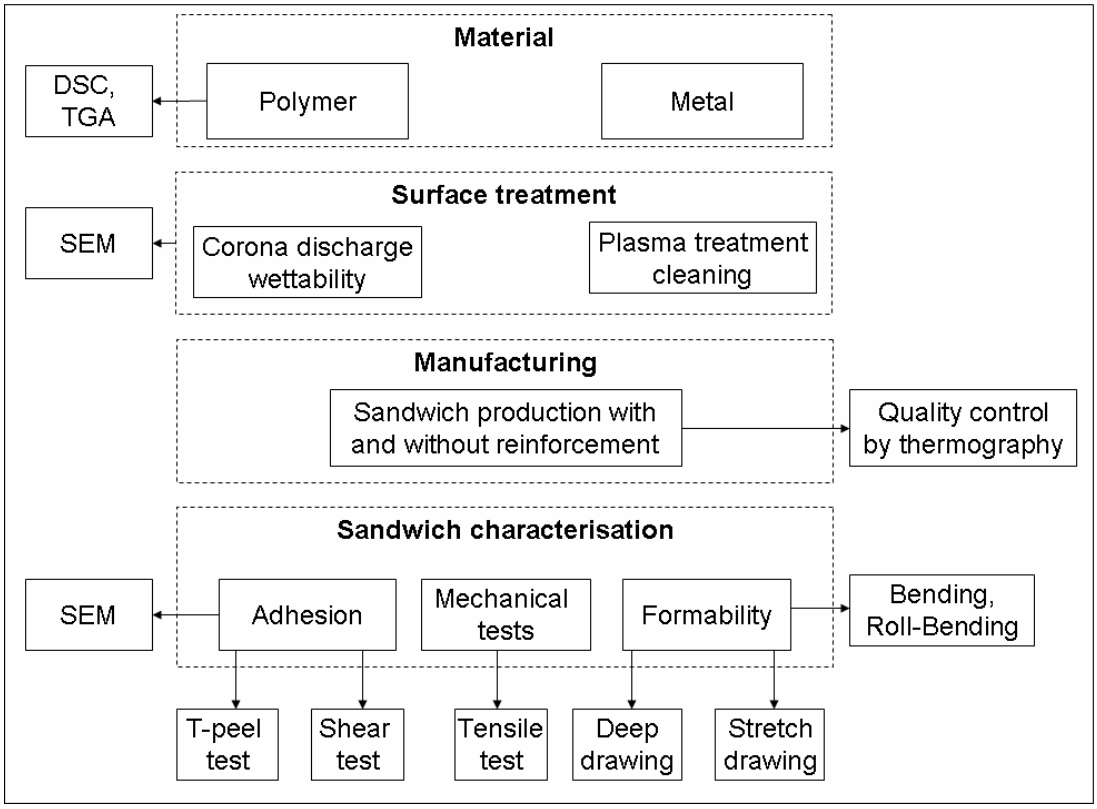

Fig. 5. Development of the project A3

Materials and Methods

Material for the sandwich production. SMS were composed of high-grade austenitic stainless steel (316L) sheets with a nominal thickness of 0.5 mm. The core consisted of a 0.6 mm thick polyolefin foil, being a mixture of polypropylene (PP) and polyethylene (PE) polymers and talc ($Mg_3Si_4O_{10}(OH)_2$), rutile (TiO_2) and barite ($BaSO_4$) (0.6 mm thick). As adhesive for bonding the layers the commercial epoxy resin Köratac® FL 201 (Kömmerling) was used.

Material for sandwich with local reinforcement. For the local reinforcing elements (RE), stainless steel 316L and steel mesh sheets with a mesh-size of 3×3 mm have been used. The thickness of the steel plates for the reinforcement was 0.5 mm. In order to determine the geometry of the local reinforcement, some simple forms for local inlays were used. The parameters of the local reinforcements are listed in Table 1.

Table 1. Materials and parameters of reinforcements for SMS

	Parameters	
Solid steel plate	Steel 316L	
Mesh steel plate	316L, size of mesh: 3 × 3 mm²	
Thickness	0.5 mm	
Geometry	Circular, square, rectangular	
Size of inlays	Circular:	Ø 36, Ø 40, Ø 50, Ø 60 mm
	Square:	36×36, 50×50 mm²
	Rectangular:	36×10, 36×12 mm²

Fig. 6 a-d depicts the central position of circular reinforcements with different sizes of the inlays within the profile of the CAD constructed sandwich cup following a deep drawing test. Due to the different inlay sizes, it is possible to determine the influence of geometry and dimensions of RE´s (content of metal and polymer material in sandwich core) on the forming behaviour of sandwich materials. For example, Fig. 6 a shows the position of RE´s edges in the transition region "head-edge" of the cap. Other examples of RE position ("edge-region" of cap) are presented in Fig. 6 b and 6 c. Fig. 6 d shows the case in which the inlay assumes almost the whole area of the sandwich sample under drawing tension.

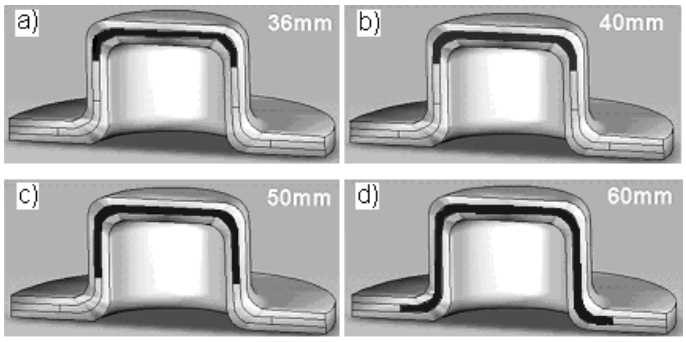

Fig. 6. Position of circular inlays with Ø of 36, 40, 50 and 60 mm. Punch Ø 33 mm, circle blank Ø 68 mm

In order to determine the bonding quality or defects in the SMS quality-control tests were employed using lockin thermography [44, 46]. This is a non-destructive test generally used to visualize the heat flow within a specimen. The heat is produced using a pulsed or sinusoidal modulated heat source to reveal concealed material characteristics or defects by means of an IR-camera. Fig. 7 a gives an overview of the arrangement, showing the high-power lamps on top, the back of the thermocamera in front and the black coloured sheet on the right side. The depth range

for analysis can be adjusted by changing the modulating frequency, amplitude and saturation of heat generation thus adapting to different kind of material or test situations (Fig. 7 b).

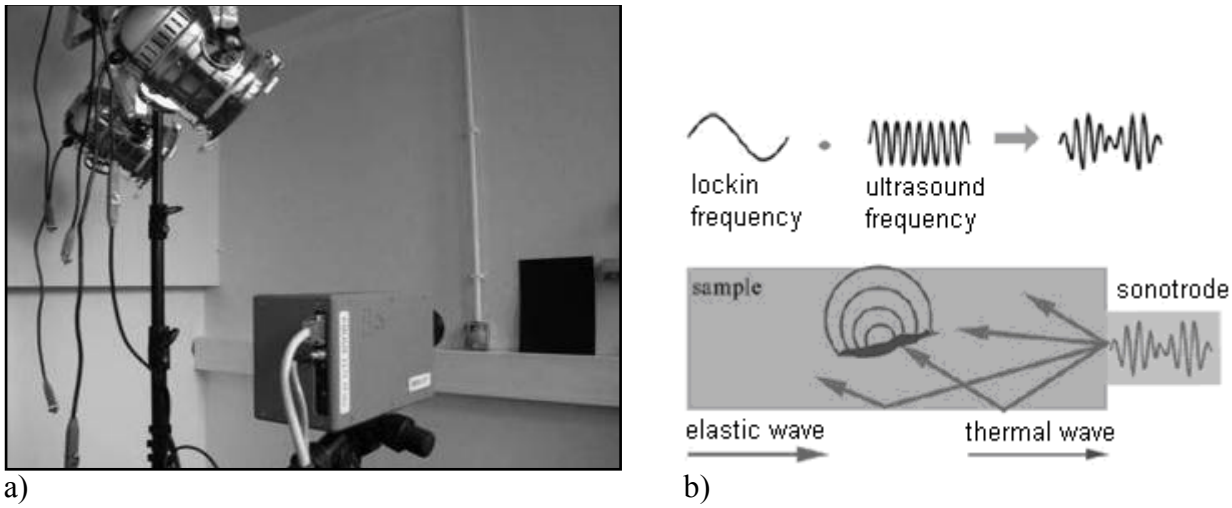

Fig. 7. Lockin thermography system (a) and process (b) [44]

During the production of sandwich materials, defects may be unintentionally introduced, such as scratches, particles or small air bubbles as well as defects depending on the RE-position (displacement of the RE's, overlapping the polymer foil, cavities around of RE etc). These defects could decrease the bonding capacity, the mechanical properties and, in general, the overall quality of the sandwich materials. The thermography equipment for controlling the samples' quality is able to analyse the size, dimension, and location of defects. Fig. 8 shows, as an example, different defects which were detected and could be analysed. In the first case (Fig. 8 a), circular inlays with a diameter of 36 mm can be seen in the sandwich core, where the upper represents a solid RE and the lower a mesh. This defect is revealed using 0.5 Hz and 100 % of amplitude. The delamination around the circular reinforcement in the upper zone is shown by the lighter coloured region around the inlays. This delamination effect can be caused by the polymer foil not being in close contact with the cover sheet during the rolling process. The reinforcement thickness in this case was 0.6 mm and the thickness of polymer foil subsequent to production by RB is about 0.5 mm. This delamination phenomenon of sandwich layers using RE with thicknesses of about 0.6 mm led to the decision only to use reinforcements with a thickness of 0.5 mm, because the very soft polymer foil reduces its thickness from 0.6 mm to 0.5 mm during the roll-bonding process.

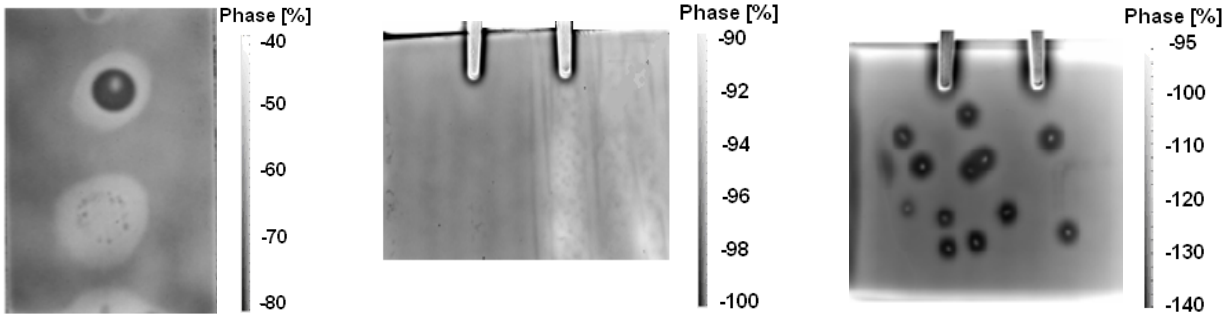

a) Delamination effect around solid (upper) and mesh (lower) steel reinforcement

b) Adhesion defect (on the right side of the sample)

c) Metal particles (inserted) as defects between core and cover layers

Fig. 8. Local defects inside sandwich composites, obtained by using lockin thermography system: a) amplitude – 100 %, frequency - 5.5 Hz, b) 100 %, 0.1 Hz, c) 100 %, 0.03 Hz

Fig. 8 b shows defects caused by excessive amounts of epoxy resin on the right side. In this case, measurements were taken at 0.1 Hz and 100 % amplitude. The final example, depicted in Fig. 8 c, is a case of powder defects between the cover and core sheets. The thermographic investigations of different kinds of defects allow a good combination of parameters to be obtained which enables the optimum quality measurements of sandwich samples to be made.

In Table 2, the experimentally chosen parameters for lockin thermography to detect specific defects are presented.

Table 2. Lockin thermography analysis of different sandwich defects according to the different frequency and phase; (-) no appearance, (o) low appearance, (+) good appearance and (++) very good appearance.

		Frequency [Hz]						
Defect thickness		1.00	0.50	0.30	0.10	0.03	0.01	0.05
Adhesive	*≈ 0.022 mm*	-	+	+	++	+	+	o
Plate Inlay	*0.5 mm*	-	++	+	+	++	+	+
Wire	*0.3 mm*	o	o	o	o	+++	+	-
Mesh inlays	*0.5 mm*	-	-	-	++	+	+	+
Al-foil	*0.02 mm*	o	o	+	++	o	o	o
Powder	*1.0-3.0 mm*	o	-	-	+	++	+	+
Phase		XX/90	-40/-80	-60/-90	-85/-95	-90/-110	-90/-120	-90/-120

DSC-TGA characterisation of core material. The thermal decomposition was studied by means of Differential Scanning Calorimetric analysis (DSC) and Thermo Gravimetric Analysis (TGA). DSC analyses were performed on a SDT Q600.

The DSC curve of polyolefin, as shown in Fig. 9, has an exothermic melting peak with an onset at 122 °C followed by a large exothermic peak with an onset at 162 °C due to decomposition. TGA shows a sharp decomposition, starting at 262 °C. The weight loss at 500 °C was 85 %. 15 % are due to the degradation of inorganic fillers such as talc, rutile and barium sulphate used by the industry. This test confirms that the choice of this PP-PE was well adapted for the temperature range. This shows the maximum operating temperature for the roll-bonding process. For this reason, the heating temperature T ~ 120° was chosen for the sandwich production.

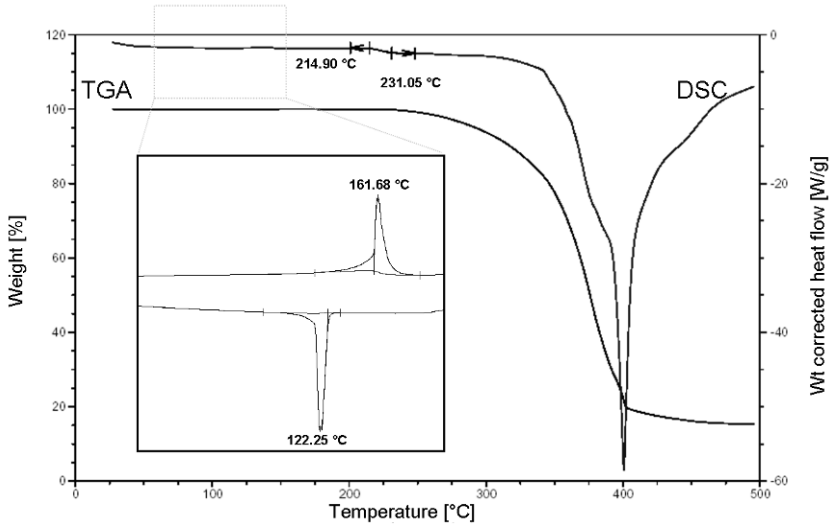

Fig. 9. Thermo gravimetric and differential scanning calorimetric analysis of PP-PE core for sandwich structures core [17]

Manufacturing method of SMS. Sandwiches were manufactured in the laboratory using the roll-bonding process (RB) [15, 16]. The RB manufacturing method is a continuous process, as sketched in Fig. 10 and can be divided into two steps:

In the first step, the metal sheets are degreased and cleaned with acetone and then coated with epoxy resin before being placed in a stationary convection furnace (1) and heated up to (265 ± 2) °C for 180 s to activate the adhesive. Simultaneously, the PP-PE foil is placed in a second furnace (2) at a temperature of (120 ± 2) °C, also for 180 s. After activation, the upper sheet metal was joined with polyolefin foil using a 2-high 12”-rolling mill (Fig. 10).

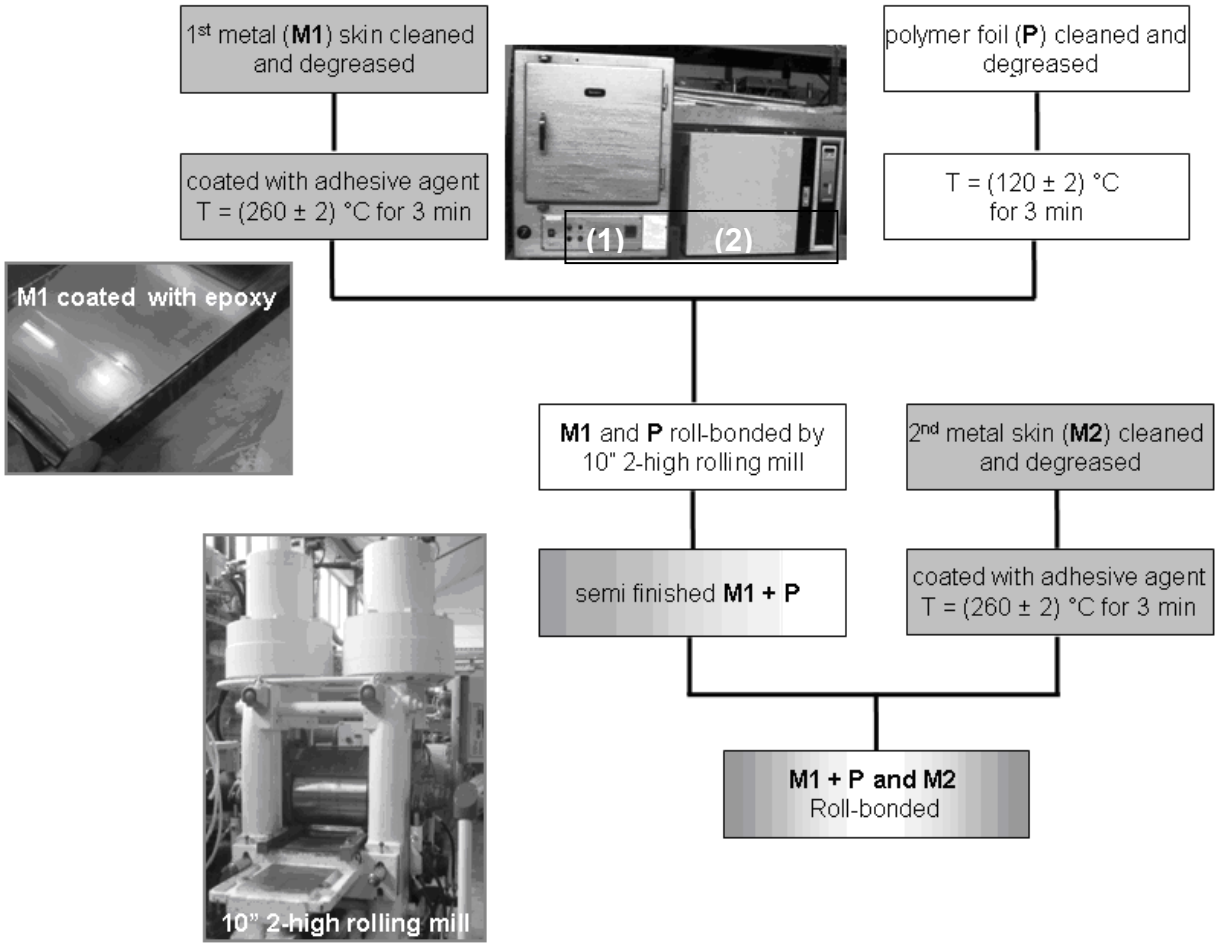

Fig. 10. Laboratory roll-bonding process

During the second step, the produced semi-sandwich is bonded to the second sheet metal, also by rolling corresponding to Fig. 10, lower part.

In order to avoid delamination between the sandwich layers, the thickness of the reinforcement was selected to be 0.5 mm. This selection depends on the assumption that during the bonding process, the soft polymer core with a thickness of 0.6 mm is being elastically and plastically deformed during the RB process. The industrial manufacturing process for reinforced sandwich laminates can be carried out as a normal RB process whereby the local reinforcement is located within form-like cavities in the polymer core whose sizes are equal to the sizes of the inlays.

Surface treatment: Corona discharge treatment for polymer surfaces. The corona equipment [47] consists of a power supply, a high frequency generator, a control box and a corona and plasma station. For the present study, an ozone gas is ionized by applying a high potential (15 kV_{max}) between two electrodes, thus creating a discharge and an electron → ion → radical bombardment of the surface with very high kinetic energies. In order to avoid the system short circuiting, a dielectric barrier was placed between the electrodes and alternating the current at a resonant frequency.

In order to obtain a full ionization (ozone gas ionized) of the gap between the electrodes, the distance between the electrode and the specimens was set to 10 mm.
For corona discharge treatment the equipment was operated at 13 kV with a variable resonance frequency in the range of 20 kHz, voltage 13 kV, power 180 W and amplitude 75 % and for plasma treatment typically was 500 W, 28 kV, 20 kV, 100 % [48].
PP-PE and 316L were treated for 20, 60, 120 s. All Corona and plasma treated samples were analysed using microscope "Cam Scan Siemens" by using the magnifications of 500X and 5000X. The polymer surfaces had to be gold coated for the examinations (Fig. 11). Three samples of treated mono-materials ($0.6\times1.5\times1.5$ mm^3) were prepared for each test. The metal surface observed by SEM is shown in Fig. 12.

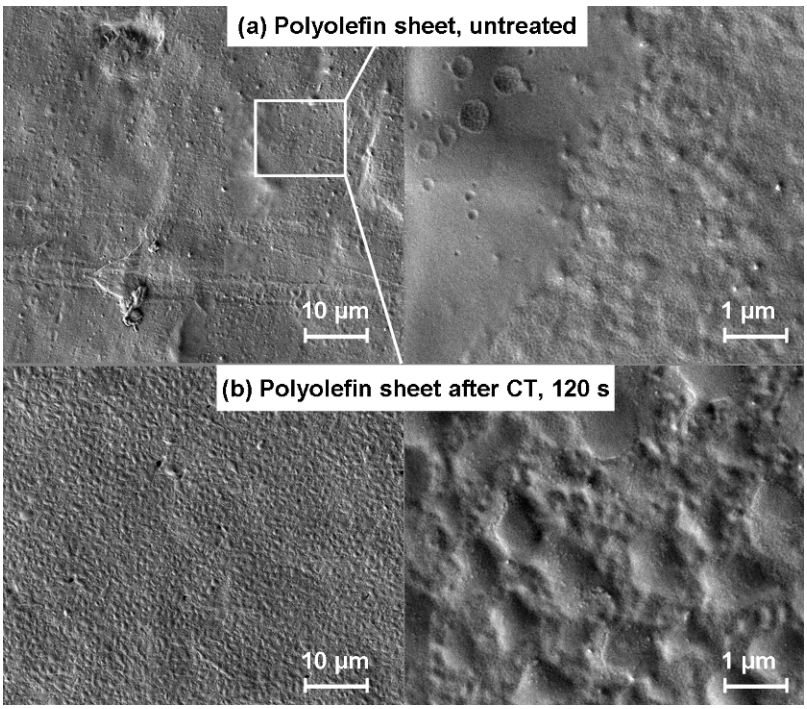

Fig. 11. SEM image of PP-PE before (a) and after (b) corona discharge treatment after 120 s. (CT = corona treatment) [50]

The effect of corona treatment on the morphology and wettability of the surfaces has been experimentally proven. The SEM images of the PP-PE films show significant changes of the surface morphology induced by the corona treatment (Fig. 11 a and 11 b). Holes (pores) and an irregular porosity distribution can be detected, which are important for the adhesion properties as shown by Tsai [49]. Indeed, as high energy particles bombarded the PP-PE sheet during treatment, small micro pits can be formed. These micro pits are microscopic holes excavated by the charges. Micro pitting can lead to increased adhesion due to a larger potential bond area. After corona discharge treatment, PP-PE's SEM images exhibit a large density of pores, an "etched character" with an irregular shaped structure and a bubble-like surface texture surrounding the pores, as can be seen in Fig. 11 a and b.

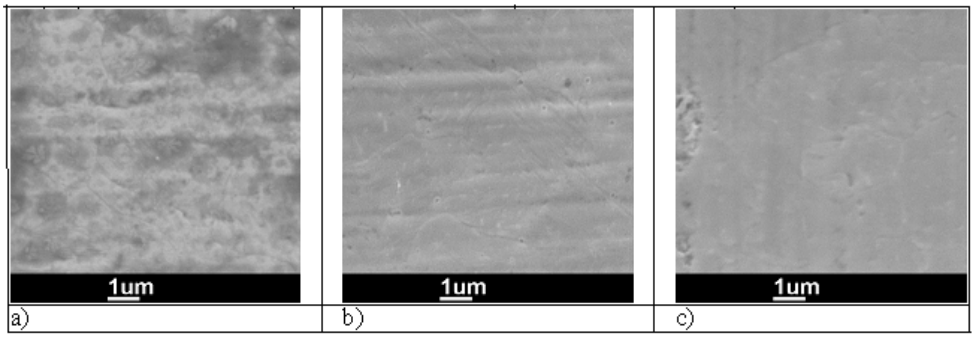

Fig. 12. SEM micrographs of untreated steel (a) in comparison with corona (b) and plasma (c) treated steel.

The comparative analysis of the corona and plasma action on the steel sheets (Fig. 12) shows that the effect of steel surface cleaning by plasma after 20 s is much more intensive than for corona treatment after the same time. However, the surface cleaning can also be seen after a 20s-corona treatment. The differences obtained can be explained by the differences in treatment temperatures after 20 s of corona (≈ 25 °C) and plasma (≈ 150 °C). On the other hand, some polymer surface defects could be detected appearing as wavy lines. They can be correlated to the plasma´s hot beam. According to the previous results, it was recommended to use the plasma treatment for steel sheets and the corona treatment for the polymer foils for future investigation and possible industrial applications.

Adhesion: (180°) T-peel and shear test

The adhesion between the polymer core and metal sheets was investigated using a universal materials testing machine and (180°) T-peel tests, according to DIN 53281-2 [51, 52]. The test serves to determine the resistance of metal bonds to peeling forces. A characteristic chart for such a test is given in Fig. 13. The dimensions of the SMS specimens were 170 mm × 30 mm × 1.6 mm. Six samples generally were used and the results were averaged for each data point [53]. Peel tests do not provide absolute material data, but it is primarily used for the comparative assessment of adhesives and adhesive bonds.

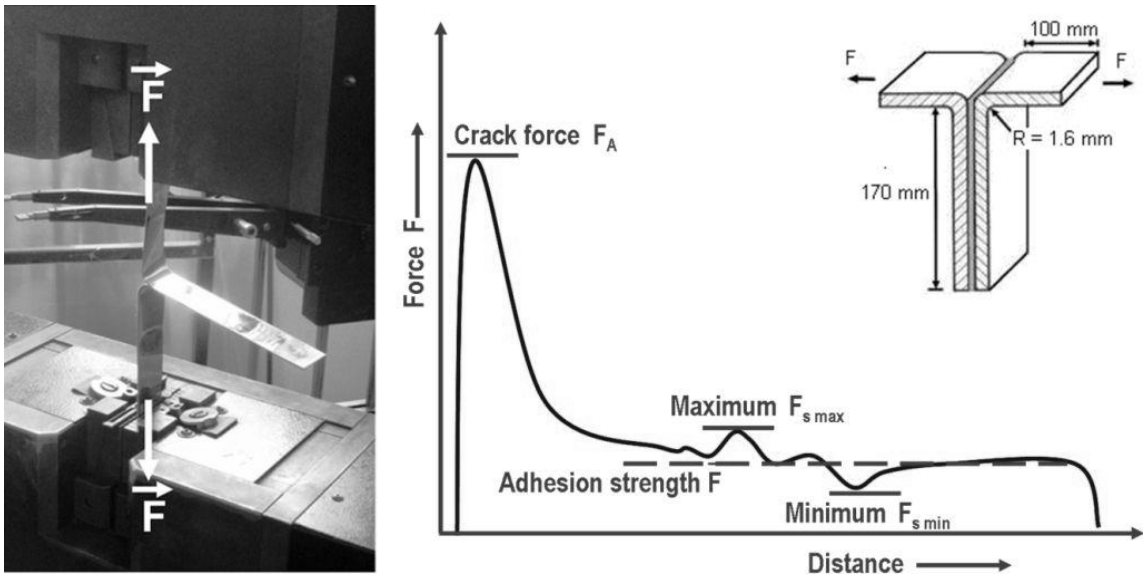

Fig. 13. T-peel test according to DIN 53282

With the crack force - peeling load - (F_A) the initial crack peel resistance – crack strength - (P_A) is defined as

$$P_A = \frac{F_A}{b} \text{ [N/mm]} \quad (1)$$

where b is the sample width (here: b = 30 mm).With the mean peel force $\overline{F}$ (adhesion strength, see Fig. 14) the mean peel resistance P_s can be defined as

$$P_S = \frac{\overline{F}}{b} \text{ [N/mm].} \quad (2)$$

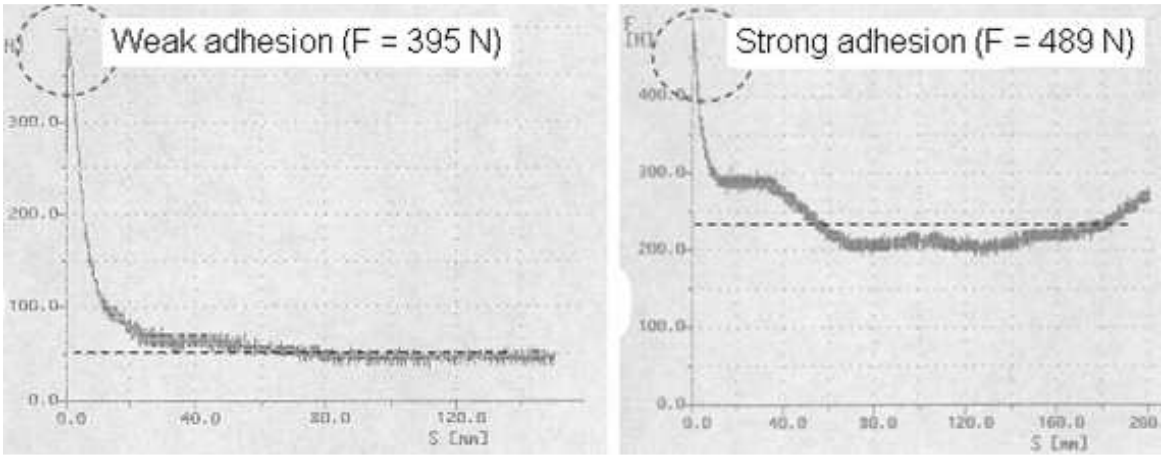

a) b)

Fig. 14. Typical curves of 180° T-peel test for SMS with weak adhesion (a) and strong adhesion (b)

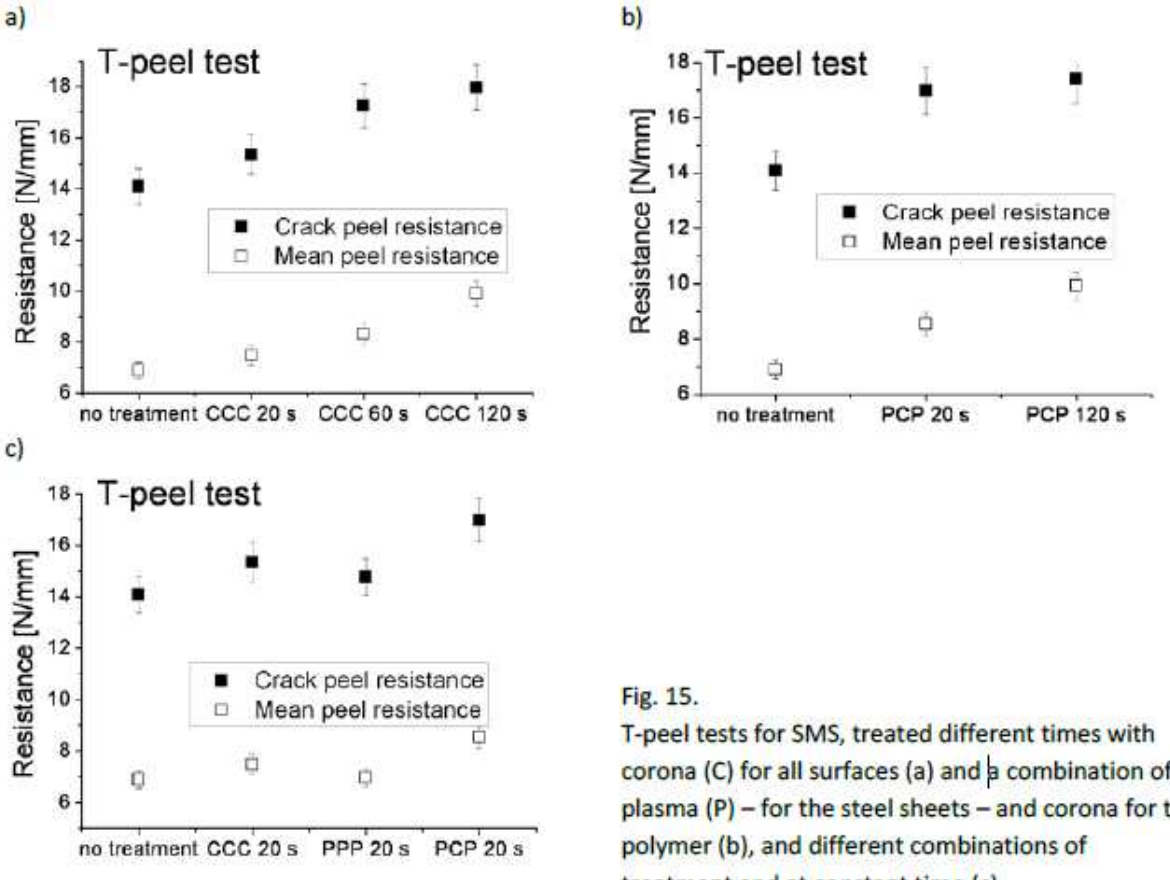

Fig. 15.
T-peel tests for SMS, treated different times with corona (C) for all surfaces (a) and a combination of plasma (P) – for the steel sheets – and corona for the polymer (b), and different combinations of treatment and at constant time (c)

The relation between crack peel resistance and mean peel resistance depends on the mechanical properties, such as Young's modulus and shear modulus or yield strength, and on the dimensions of the specimens.

Typical curves obtained for SMS with low (a) and high (b) adhesion are presented in Fig. 14. The maximum crack peel force (≈ 390 N) (circled) and the level of the mean peel force (≈ 52 N) is depicted for a weak bond in Fig. 14a. The peel resistance for this type of sandwich is low. For a good bonding Fig 14 b, the results of the T-peel test show a strongly increased force level with a maximum crack peel force of about 490 N and a mean peel force about 235 N.

A summary of the results obtained by the T-peel tests for differently treated SMS are presented in Fig. 15. Fig. 15 a represents the results for corona treatment on steel and polymer surfaces for different times, Fig. 15 b shows the data for a combined treatment and different times, Fig. 15 c compares the results of different treatments at 20 s treatment time. SMS without surface treatment shows the crack peel resistance of 14.5 N/mm. By an increasing the corona time from 20 s until 120 s (Fig. 15 a) the crack peel resistance is also increased from 15.4 N/mm up to 18.0 N/mm. This effect is also observed by the combined treatment of plasma and corona (Fig. 15 b and c). The same tendency can clearly be seen with mean peel resistance.

The shear tests were carried out using a universal materials testing machine, according to [54]. The 200 mm × 30 mm × 1.6 mm SMS have opposite notches with a displacement of 10 mm as been sketched in Fig. 16. The shear area was 300 mm² and the cutting clearance was 2.5 mm.

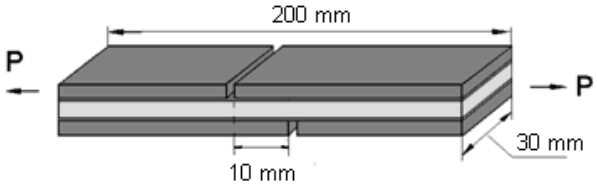

Fig. 16. Sample geometry for the shear-test

The shear resistance (P) is defined as

$$P = \frac{F_{\max}}{A} \text{ [N/mm]} \tag{3}$$

where, F_{max} is the maximum crack force by shear test, and A is the shear area of specimen between the notches. Five samples were used for differently treated sandwich materials. The results were averaged for each data point. Primarily the test was developed and used to determinate the shear strength of different layers in fibre reinforced composites.

a) b)

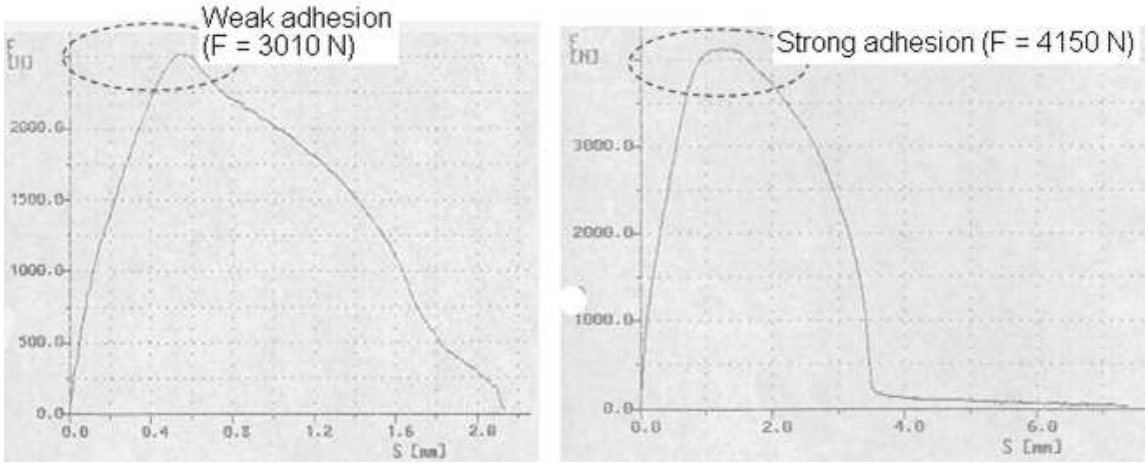

Fig. 17. Shear test a) for SMS with a weak adhesion (a) and a strong adhesion (b)

Fig. 17 depicts two typical curves obtained following the shear test on SMS with a weak (a) and a strong (b) adhesive resistance. The maximum shear force for the sandwich with a weak bonding is about 2500 N (circled), see Fig. 17 a, and the maximum shear force for a sandwich with good bonding properties, approximately 4100 N, is demonstrating the high adhesion of that sandwich, Fig. 17 b.

As shown in Fig. 11b, corona treatment changes the surface morphology. Roughness is increased by means of the surface activation. Moreover, the corona treatment's oxidation process strengthens, prepares and improves the epoxy resin's adhesive behaviour. As demonstrated, the effect of corona strongly depends on the treatment times (Fig. 15 and 18).

Fig. 15 shows a strong increase in crack-peel resistance (28 %) and mean peel resistance (43 %) with increasing corona exposure time from 20 to 120 s. Moreover, an improvement of the shear resistance (22 %) is measured following corona treatment. A linear tendency of improvement is observed in either Fig. 15 or Fig.18. These results can be explained by the creation of polar chemical functional groups due to the corona surface treatment. They enhance the surface adhesion and wettability as stated by Zhang [22], too.

The experimental results obtained by shear tests for the SMS, treated for different times of corona and plasma discharge, are shown in Fig. 18. For corona treatment of all surfaces increasing of exposure time leads to an increase of the shear resistance of the sandwich (Fig 18 a). Comparing plasma with corona treatment for an exposure time of 20 s on polymer surface the PPP treatment shows a slightly reduced value due to the strongly heating up of the polymer (above melting temperature) by the plasma treatment. The combination of plasma – for steel surface – and corona – for the polymer – improve the shear resistance clearly as can be seen in Fig. 18 b. A PCP-combination leads to an increase of shear resistance with increasing treatment times (Fig. 18 c), as could been expected from Fig. 18 a and b.

a)

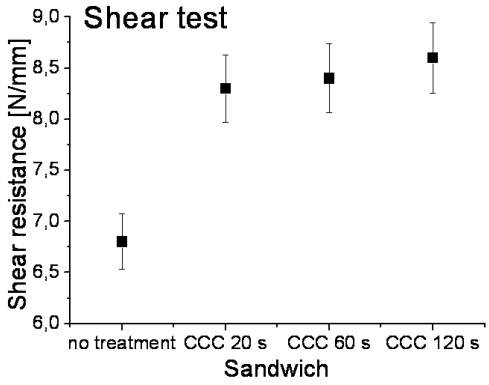

b)

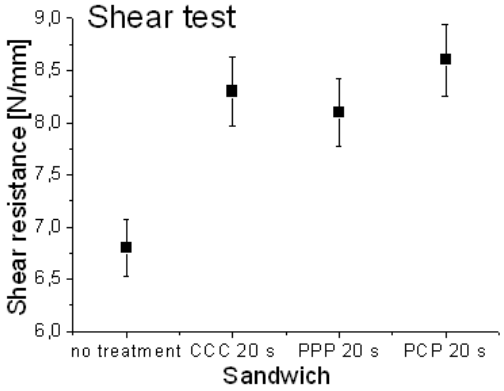

c)

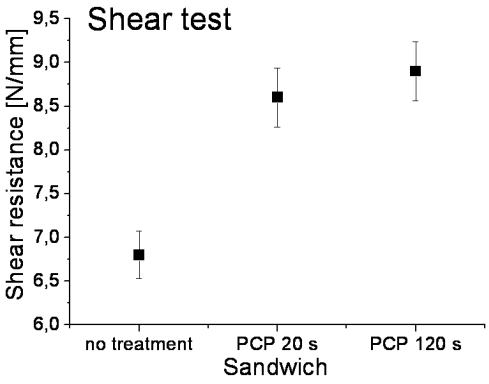

Fig. 18.
Shear resistance for 316L/PP-PE/316L SMS
(a) after corona (C), (b) after combined corona and plasma (P) treatment and (c) for different exposure times

The results obtained by shear tests for the sandwich materials treated by corona and plasma show quite similar adhesion strengthening effects and a quite constant shear resistance of 8.5 N/mm. The sandwich samples without treatment have a clearly lower shear resistance value of about 7 N/mm.

The corona discharge in combination with plasma treatment for the metal surfaces can be used to improve the wettability and adhesion properties of metal-polymer-metal sandwich materials.

Mechanical characterisation

Tensile test. To measure the yield strength (YS), tensile strength (TS) and elongation to rupture (ER), tensile tests were carried out using a universal testing machine with an initial strain rate of 1.67×10^{-3} s^{-1} for metal sheet, polymer foil and SMS. Therefore tensile specimens with a gauge length of 120 mm were prepared from the steel skin materials, the PP-PE core material as well as the steel/PP-PE/steel SMS [55]. To determine the anisotropy effects, these tests were performed taking specimens at $\alpha = 0°$, 45° and 90° to the rolling direction of the sheets. To avoid delamination at the edges by cutting, SMS samples were prepared by water-jet cutting, a suitable method for preparing these types of sandwiches. The metal samples were cut using a standard stamping tool.

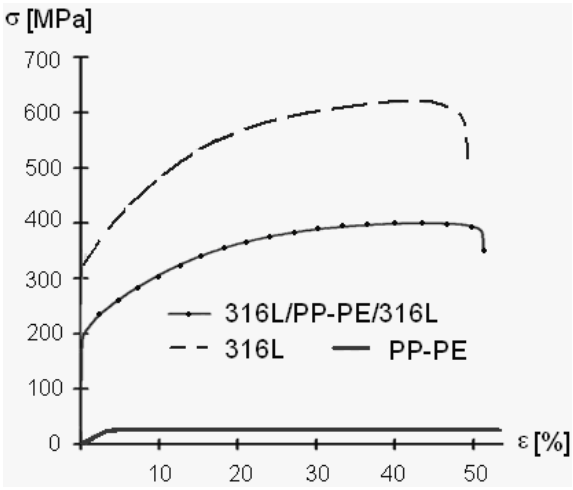

Fig. 19. Stress–strain curves for the stainless steel (316L), SMS and polymer sheet (PP-PE) at room temperature transversal to RD of the sheet

As an example, a comparison of SMS and with monolithic materials is given in Fig. 19 where tensile tests were carried out transversal to rolling direction (RD) of the metal sheet and typical stress–strain curves were obtained. Under uniaxial tensile loading, the steel material and SMS show macroscopically homogeneous deformation up to the ultimate tensile strength is reached at a stress of 620 MPa and 400 MPa, respectively. Subsequent ductile failure occurs at a macroscopic strain of approximately 53 % and 50 %, respectively. Additionally, the tensile test summarizes the mechanical properties of the steel skin, the PP-PE core and the SMS and shows the reduction in yield stress (Table 3) following the rule of mixture for flow stresses of the sandwich sheets. Eq. 4 gives the proportion, where σ and V indicate the uniaxial flow stress and volume fraction, and subscripts SMS, M and P represent the sandwich sheet and its layers “M” metal and “P” polymer, respectively.

$$\sigma_{SMS} = \frac{\sigma_M \cdot V_M + \sigma_P \cdot V_P}{V_M + V_P} \tag{4}$$

Since the tensile strength (Table 3) and elongation to rupture (Table 3) for PP-PE core are of no interest in regard to the deformation used in these applications, they were not determined.

Table 3. Mechanical properties for the 316L skin, the PP-PE core and SMS, taken at room temperature and for three angles α to RD. Mean ± SD for n = 5 [56]

Sample	Angle to rolling direction α [°]	YS ± SD [MPa]	TS ± SD [MPa]	ER10 ± SD [%]
316L	0°	310 ± 1	608 ± 4	48 ± 2
	45°	313 ± 7	610 ± 9	54 ± 1
	90°	314 ± 6	618 ± 14	53 ± 1
PP-PE	0°	26 ± 1	-	-
	45°	24 ± 1	-	-
	90°	28 ± 1	-	-
SMS 316L/PP-PE/316L	0°	180 ± 18	388 ± 19	48 ± 3
	45°	180 ± 2	378 ± 4	49 ± 2
	90°	196 ± 16	400 ± 18	53 ± 3

To study the influence of corona treatment on the mechanical properties in SMS, tensile tests were carried out for 316L–PP-PE–316L sandwich sheets with a corona treatment of the PP-PE core.

The combinations of the cover sheets are sketched in Fig. 20. Version "L" characterises the roll-bonded SMS with the metal sheet rolling direction parallel to the bond rolling direction. Additionally "T" represents the SMS which has been produced turning the second metal sheet with its RD perpendicular to the RD of the first one. To determine the anisotropic behaviour, the tensile tests were performed on "L" and "T" specimens taken at α = 0° and 90° to the roll bonding direction. Because of the before mentioned reasons the samples were prepared using water-jet cutting.

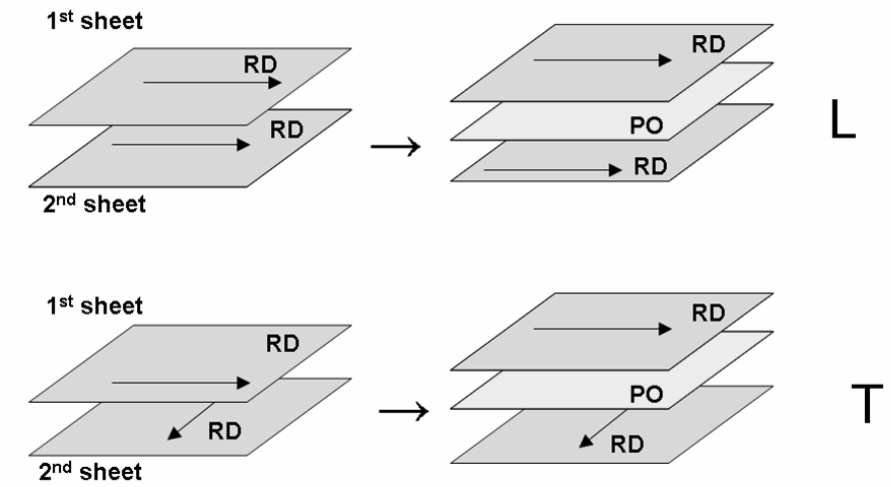

Fig. 20. Indicating the SMS with "L" and "T" in dependence on the orientation of the metal sheets

Studying the mechanical properties of corona-modified PP-PE in a SMS, it can be seen that treating the polymer core with corona in air a marginal increase in strength can be stated (Table 4). YS and TS have been found to be affected by corona treatment indicating that these composite properties were highly sensitive to interfacial phenomena. However, elongation at rupture of composites was slightly decreased after corona treatment. This follows the standard rules of mechanical behaviour. For SMS T_CT (α = 0°), a pronounced improvement of 8 % and 16 % for TS and YS could be observed, respectively.

Table 4. Mechanical properties at room temperature, for different processed SMS (see Fig. 20) under 0° and 90° to RD and with treated and untreated polyolefin. (Mean ± SD for n=3) (CT= corona treatment) [50]

SMS	Angle to rolling direction α [°]	YS ± SD [MPa]	TS ± SD [MPa]	ER10 ± SD [%]
L	0	180 ± 18	388 ± 19	48 ± 3
	90	196 ± 16	400 ± 18	53 ± 3
L_CT	0	192 ± 20	402 ± 20	43 ± 2
	90	208 ± 18	414 ± 20	48 ± 2
T	0	174 ± 17	381 ± 21	48 ± 6
	90	190 ± 21	398 ± 19	53 ± 5
T_CT	0	203 ± 20	409 ± 22	48 ± 3
	90	189 ± 20	394 ± 20	43 ± 5

Additionally, in the case of SMS L_CT (α = 0°) and L_CT (α = 90°), a slight rise of 4 % and 6 % (for TS and YS) was visible. On the other hand, for T_CT (α= 90°) no variation could be discerned. Using the CT variation, the composites' elongation at rupture did not change significantly.

Formability

Stretching and deep drawing methods. Currently, a lot of research is done on the development of forming processes for sandwich composite materials, with and without reinforcement; here especially for stretching and deep drawing. Both types of deformation are widely used for the production of automotive parts, such as body panels. The stretch forming behaviour can be characterized typically by the Erichsen test, according to DIN 50101 [57]. It is also important that the sheet can be deformed by elongation and uniform thinning and is capable to be shaped in complex 3D-structures. To determine the limits of formability for the SMS and their suitability for deep drawing this test was performed on the composite sheets and compared with the results of the mono-material. A cone-shaped spherical-ended plunger deforms the tested sheet, which is restrained around its periphery, until fracture occurs. The height of the cup at fracture (called the Erichsen index) is a measure for stretchability and a reference value for the materials (Fig. 21 a). To evaluate formability of the sheet and the SMS, additionally deep drawing tests were carried out using a deep drawing benchmark test, as shown in Fig. 21 b.

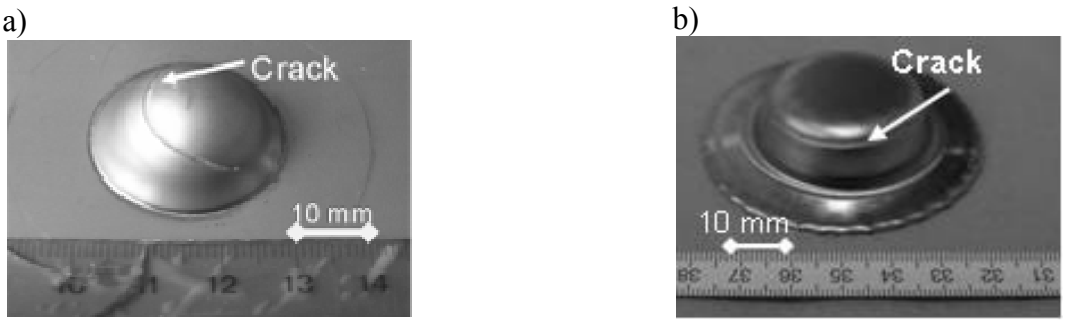

Fig. 21. Erichsen stretch forming (a) and deep drawing (b) tests

During the deep drawing process, a flat blank is clamped between the die and the blank holder. Then the punch moves down to deform the clamped blank into the desired shape. The final shape of the product is affected by the geometry of the tools, the material behaviour of the blank and the process parameters. Due to the tangential tension (σ_t), wrinkling in the flange and cup-wall fracture can occur during the deep drawing process. Fig. 22 shows the component of stress acting in the different areas due to the deformation process.

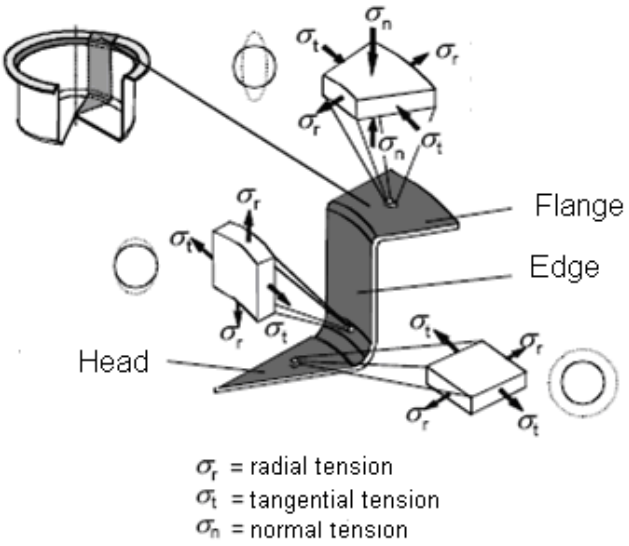

Fig. 22.Deep drawing with a flat punch and a blank holder for rotational symmetric specimen [58]

It was found that all the stresses, such as σ_r and σ_t, are produced on the edges of the punch. Owing to this, this area is considered to be the most critical region.

The parameters of the Erichsen testing equipment are presented in Table 5. In order to avoid the friction between the equipment and the tested sample, Vaseline was used as a lubricant for the drawing and stretching processes.

Table 5. Testing parameters for deep drawing and Erichsen tests with Ø 68mm blanks

		Erichsen test	Deep drawing test
v: Speed of drawing	[mm/s]	0.5	0.5
D_0: diameter of the circular blank	[mm]	68.0	68.0
d_0: diameter of the punch	[mm]	30.0	33.0
s_0: thickness of sandwich sample		1.6	1.6
μ: coefficient of friction for steel sheets		0.002....0.0025	0.002....0.0025
TS: tensile stress	[MPa]	410	410

For the deep drawing process of sandwich materials, knowledge of the blank holder pressure and force was necessary. Too small blank holder pressure increases the risk of wrinkling [58].
The blank-holder force was calculated for the 1.6 mm thick SMS using equation by Siebel [59]:

$$F_{BH}=\mu\left[\left(\frac{D_0}{d_0}-1\right)^3+0.5\cdot 10^{-2}\cdot\frac{d_0}{s_0}\right]TS \tag{5}$$

Digital image correlation method – photogrammetry. The digital image correlation method (which is also referred to as photogrammetry) has been successfully employed for the determination of the elastic–plastic displacement and strain fields in metallic materials with [60] with ARGUS® program from gom [61].

It is based on the recognition of geometrical changes in the gray scale distribution of surface patterns before and after straining. A regular dot pattern is chemically etched on the sheet metal prior to deformation. In the forming process, this dot pattern is distorted as it deforms with the sheet. The deformed sheet metal is recorded from different viewing directions using CCD cameras and program defining the centre point of all marked dots in each image. Then, using

photogrammetry techniques, the images are virtually assembled to represent the object in 3D coordinates.

From the local distortion of the regular grid pattern which was applied on the flat sheet metal, the local strain introduced by the stamping process is calculated. These strain values, which usually represent the major and minor strain as well as the thickness reduction (in %), define the degree of deformation and elongation according to v. Mises as well as Tresca (in %).

Forming limit curve (FLC). The failure of the sandwich sheet materials under different load conditions, e.g. tensile loads, had to be studied. To investigate the influence of the polymer core layer during the sandwich composite's forming process under stretching and deep drawing conditions punch-forming tests were carried out on 1 mm thick stainless steel 316L sheets and compared with the results of non-reinforced 316L/PP-PE/316L (0.5/0.6/0.5 mm) SMS.

The Nakajima test [62] is a method for determining the FLC. This test is based on the principle to deform sheet blanks of different geometries with a circular punch up to fracture. By changing the geometries of the SMS - as shown in Fig. 23 – starting from a circular plate, which is indicating the state of regular biaxial deformation, to a strongly waisted shape, representing the tensile condition– different major and minor strains can be put into relation. The manufactured SMS samples with different sizes and geometries were prepared by water-jet cut system while Table 6 shows the selected sizes and geometries of the sandwich samples.

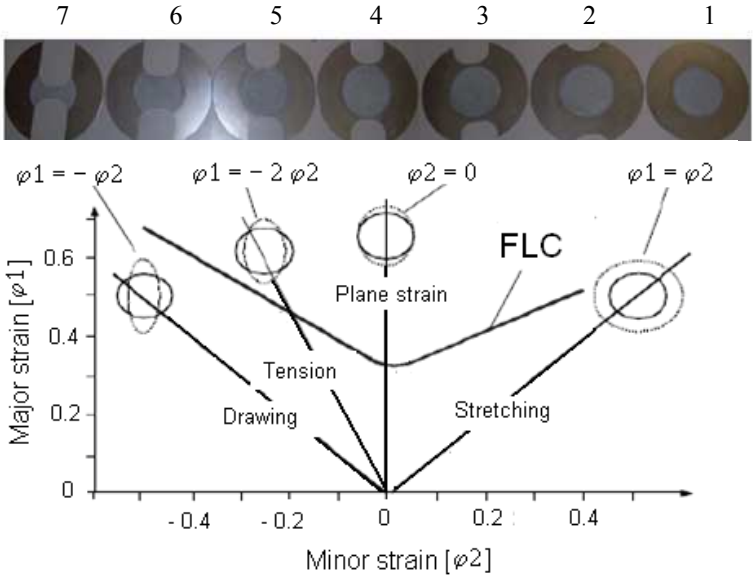

Table 6.
Dimensions of SMS and steel samples for FLD

Shape of sample	Outer diameter of sample D=180 mm	Inner "diameter" [mm]
1		180
2		140
3		100
4		90
5		80
6		50
7		20

Fig. 23. Definition of FLC and geometry of samples

To measure the main deformations and their directions photogrammetric analysis was applied [63, 64]. To follow the deformation path in every point of the surface a grid with exact and regular pattern can be used – so to measure the displacement of selected points with well known coordinates after the forming process. By subtracting the starting data from the final ones the state of deformation can be calculated. On the other hand a stochastic pattern can be created on the surface by using a white lacquer with black pigments being sprayed on. The movement of these pigments is followed during processing until fracture by an optical device delivering the data to a computer to calculate the change of position for the dots and, therewith the principle strains for the different conditions. The principle strain values provide one point within the FLD. Finally, the combination of the points defines the FLC.

The drawing tests and photogrammetric analyses' results are used to build the FLCs for a 1 mm thick steel sample and – in comparison - sandwich samples 316L/PP-PE/316L with 0.5/0.6/0.5 mm thick layers.

Fig. 24 shows that under the same geometrical – and therewith load - conditions, the level of FLC for the 316L sheet in the stretching area as well as in the plain strain area is slightly higher than that of the SMS. That means that 316L mono-material exhibits a better forming behaviour than the SMS sheets.

In the deep drawing region, the principle strain values of the SMS and 316L are approximately correspondent. Because of the polymer component in the SMS the plasticity is improved compared to the steel mono-material, especially during the deep drawing process. This may be due to the narrow width of the samples which influence the plastic deformation behaviour of the sandwich sample with polymer core.

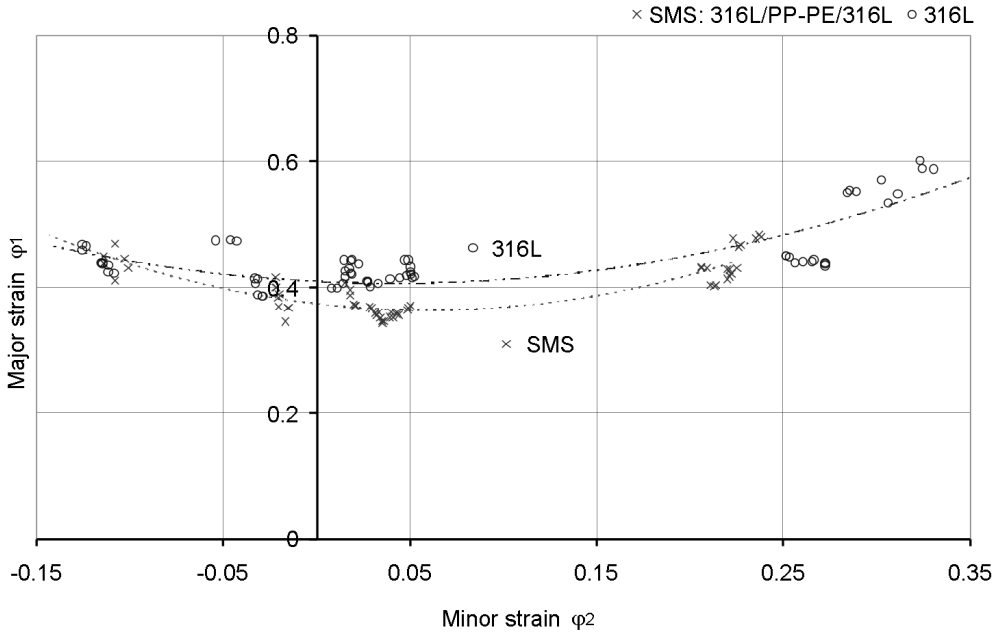

Fig. 24. FLC for sandwich composite material: 316L/PPPE/316L - and steel sheet 316L

Stretch- and deep drawing tests on SMS without reinforcement. The formability was investigated by cup stretch- and deep drawing tests using sandwich composites with and without solid and mesh steel inlays of circular and rectangular size. The parameters for stretching and deep drawing tests used are given in Table 7.

The stretch- and deep drawing tests were first carried out for various sandwiches without reinforcement produced as “L”-and “T”-type as described before. In order to compare the forming behaviour of laboratory produced sandwich samples, industrially manufactured ones (Hylite [11] and H400/PP/H400 [8]) were deep drawn parallel under equal conditions. The results for Erichsen and deep drawing tests are summarised in Table 7.

The height obtained by the stretching and the drawing processes is used to assess the formability of the tested materials. Table 7 shows that the sandwich samples, been produced in the laboratory, have a higher formability than that ones obtained from industrial production.

Table 7. Averaged maximum cup height of ten samples each in the Erichsen and the deep drawing cup test

	Erichsen test		Deep drawing test	
SMS	H [mm]	F [kN]	H [mm]	F [kN]
316L/PP-PE/316L L, Corona	11.4 ± 0.3	37 ± 2	16.2 ± 0.2	74 ± 3
316L/PP-PE/316L T, Corona	11.5 ± 0.9	38 ± 2	16.2 ± 0.3	74 ± 3
316L/PP-PE/316L L, 0°, without Corona	11.4 ± 0.5	11 ± 1	16.2 ± 0.4	72 ± 2
316L/PP-PE/316L T, 90°, without Corona	11.5 ± 0.4	36 ± 3	16.0 ± 0.3	74 ± 2
Hylite 0.3/0.9/0.3	6.7 ± 0.9	7 ± 1	10.4 ± 1.2	21 ± 1
H400	10.5 ± 0.7	21 ± 3	6.7 ± 0.3	7 ± 1

Comparison between industrially and laboratory roll bonded sandwich

To analyse stretching and the forming behaviour, Erichsen and deep drawing tests have been performed with different skin materials and their combination using the same core. Comparison was made for roll bonded SMS with the pure metal sheets and the industrial one (Table 8). Furthermore, morphological observations were performed on sandwich cross-sections and investigated by using of a field emission microscope JEOL JSM-6700F in order to observe the metal skin/polymer core interface.

Table 8. Skin layer composition and SMS thickness

Abbreviation	Specimen	Total thickness [mm]	Process
Steel	Steel 316L (1.4404)	1	-
IND1	H400 (1.4376; PP-PE)	1.6	Industrial
SRB1	1.4404/PP-PE/1.4404	1.5	RB
SRB2	1.4404/PP-PE/AlMg3	1.5	RB
SRB3	AlMg3/ PP-PE/1.4404	1.5	RB
SRB4	AlMg3/PP-PE/AlMg3	1.5	RB
AlMg3	Aluminium alloy	1	RB

The polymer core of 316L/PP-PE/316L (Fig. 25, left) is compact. In the PP-PE core, talc foils; rutile and barite particles are visible in the cross section. On the other hand, some air bubbles are visible in the polymer core of H400 (Fig. 25, right). The epoxy resin between the metal skin sheet and polymer core can be observed to improve their adhesion. No micro cracks or delamination were observed.

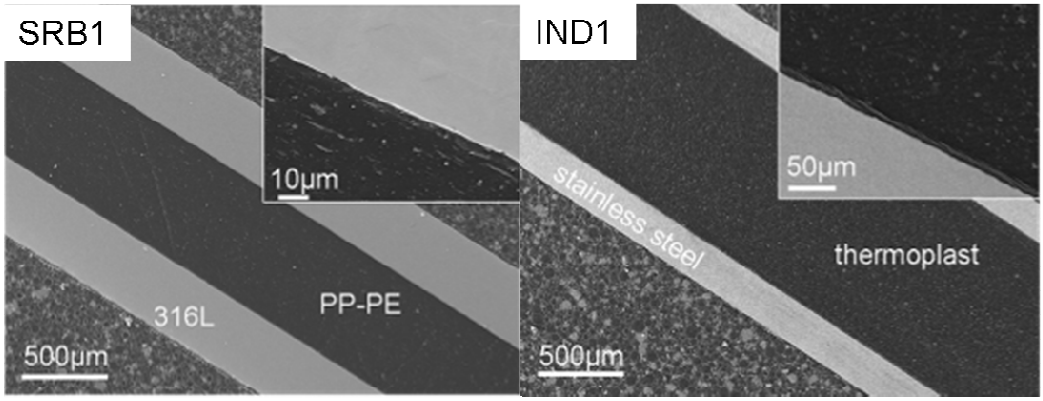

Fig. 25. Cross-section of sandwich SRB1with PP-PE core (left) and of industrial one IND1 (right) [16]

The results of the Erichsen tests performed confirm the improved behaviour of laboratory produced SMS (SRB1) compared to the industrially produced SMS (IND1), and come close to the value of the monolithic material (steel) (Fig. 26 a). Even the combination of Al- and steel-alloys as skin material (SRB2) shows a better value than IND1. The value for SMS with Al-skin (SRB4) is close to that for the monolithic material (AlMg3).

The results for deep drawing tests for the above mentioned SMS are presented in Fig. 26 b, and show the same relations as previously discussed for the Erichsen test: SRB1 with steel sheets as skin layers attained the greatest depth, approximately 74 mm, without wrinkling and fracture. This comes close to the value of the monolithic material. On the other hand, in the case of SRB2 and SRB3, Al-alloy as one layer of the cup and steel as the other layer, some wrinkling appeared. To avoid this phenomenon, a higher blank clamping pressure was chosen which lead to reduced drawing depths (from 70 mm to 64 mm). The values obtained from the laboratory SMS were comparable or even showed improved values to the industrially produced SMS and monolithic materials. It can be stated that this laboratory process is suitable to produce SMS in a good quality. The roll bonded SMS show great potential in drawability.

(a) (b)

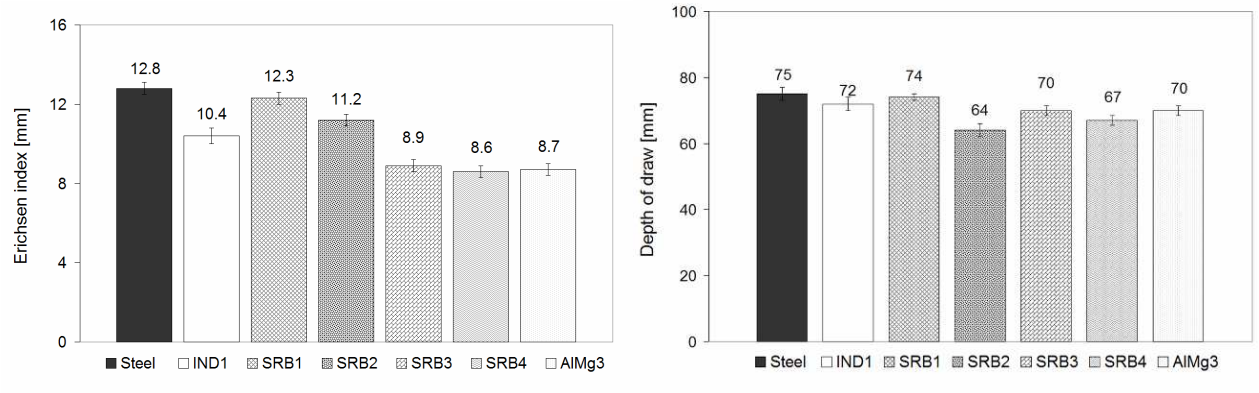

Fig. 26. Averaged maximum index of five samples in Erichsen test (a); comparison of different SMS by deep drawing test (b). Data: mean ± SD (n = 5)

Stretching and deep drawing tests of SMS with reinforcement

In order to obtain the influence of different reinforcements (material, shape, dimensions) on the formability of metal-polymer sandwich materials, five samples from each kind of sample were analysed by stretch and deep drawing processes. All experimental results were averaged. The deep drawing and stretching processes were carried out up to crack initiation. The position in these first investigations was kept central; the sizes of the inlays were changed between Ø 36 mm to Ø 60 mm, as sketched in Fig. 27.

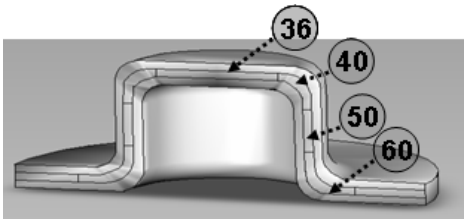

Fig. 27. Circle reinforcement with 36, 40, 50 and 60 mm^{Ø}

Table 9 resumes the results of deep drawing tests performed on sandwich composites without inlay compared to those ones with circular and rectangular inlays from solid steel and mesh steel sheets. Drawing force augments for samples with the insertion of different size inlays compared to sandwich laminate without inlay. The only exception could be found with an inlay of Ø 60 mm (66 kN). By drawing sandwiches with a reinforcement of Ø 60 mm, a delamination was observed in the blank holder area and the cracks initiate normal to the region "head-wall"; this means that the limit was reached where the area of the reinforcement was such big that the non-reinforced could not keep the stresses and delaminated. So, under these conditions an upper limit seems to be given by reaching a share of about 80 % of the sandwich specimens overall area for the reinforcement.

Table 9. Stretching and deep drawing tests until failure. H, cup height and F, force. The data represent the mean ± standard deviation for n=5. * = cracks in region "head-edge"; # = delamination [65].

		Deep drawing			stretching drawing	
Type of inlay	Inlay size [mm]	H [mm]	F [kN]	Failure behaviour	H [mm]	F [kN]
	no inlay	16.2 ± 0.4	72 ± 2	*	11.5 ± 0.4	36 ± 3
Circle, solid steel	Ø 30	14.7 ± 0.3	72 ± 3	*	–	–
	Ø 36	13.0 ± 0.1	73 ± 2	*	11.2 ± 0.3	42 ± 2
	Ø 40	13.5 ± 0.6	76 ± 4	*	–	–
	Ø 50	15.3 ± 0.4	77 ± 1	*	12.5 ± 0.3	47 ± 4
	Ø 60	12.4 ± 0.9	66 ± 4	* and #	–	–
Circle, mesh steel	Ø 36	13.3 ± 0.3	66 ± 3	*	10.4 ± 0.4	42 ± 1
	Ø 50	15.7 ± 0.2	76 ± 4	*	12.5 ± 0.5	46 ± 2
Rectangular, solid steel	36×36	11.7 ± 0.8	72 ± 4	*	11.7 ± 0.3	–
	36×20	11.9 ± 0.6	71 ± 1	*	12.0 ± 0.2	–
	36×10	12.6 ± 0.8	71 ± 3	*	12.6 ± 0.1	–

For sandwich composites, reinforced by circular inlays, the measured depth of deep drawing grows with increasing diameter of inlay, though their values are slightly smaller compared to non-reinforced SMS. This can be explained by an increment in the reinforcement material's working area, and the different tensile stress concentrations corresponding to the reinforcement's edges placed in the zone of maximum stress, while the 50 mm diameter inlay disks exceed that zone leading to a step-up of the height. Sandwiches with 30 mm of inlay exhibit the higher values of forming in the edges because of soft polymer presence in high concentrated transition region of the cup.

To reduce the weight of sandwich some mesh steel inlays were chosen according to the circle geometry of inlays with diameters of 36 mm and 50 mm leading to a rising in cup height of about 3% (Ø of 36 mm) and about 5% for Ø 50 mm compared to solid steel reinforcements.

The results for solid steel reinforcements with sizes of 36×36 mm, 36×20 mm and 36×10 mm are presented in Table 9. Focusing on sandwiches with square plates it can be seen that size 36×36 mm exhibits a maximum cap height of 11.7 mm; reducing the dimension to 36×10 mm, the expected slight increase in the cup height is detected.

By changing the shape from square to rectangular form the cap height increased due to the growth in the amount of polymer being drawn.

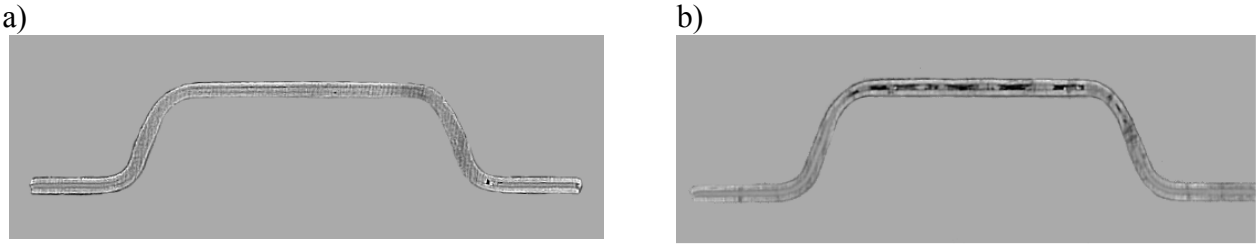

Fig. 28. Metallographic intersections of reinforced sandwiches with solid circle (a) and mesh steel circle (b) of Ø 36 mm. Size of mesh is 3x3 mm.

To understand the flow behaviour of the cover sheets depending on different types of the reinforcements, SMS were provided with different centered reinforcements, as shown in Fig. 28, and drawn to different cup heights. As an example the thickness reduction of sandwich composites without inlay (Fig. 29 a), with inlay of Ø 36 mm (Fig. 29 b), and with mesh steel inlay of Ø 36 mm(Fig. 29 c) are compared after a deep drawing depth of 10 mm by photogrammetry.

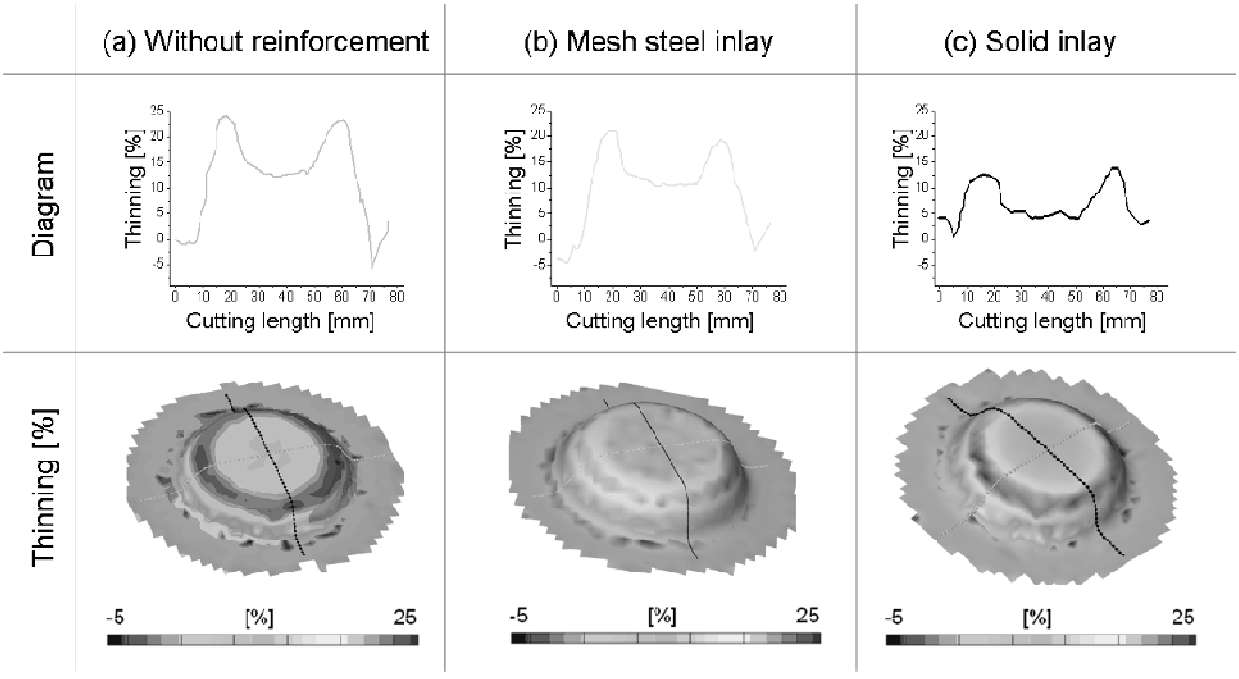

Fig. 29. Thinning of 316L/PP–PE/316L SMS without (a) inlay and with Ø 36 mm mesh (b) and solid (c) steel inlay. Plot of diagram following data along black line

Compared to the solid steel inlay, the sandwich with mesh inlay shows higher degree of thinning at the outside (21% vs. 15%). Because of the missing stiffening effect the non-reinforced sandwiches exhibit the highest deformation with a thinning about 25%.

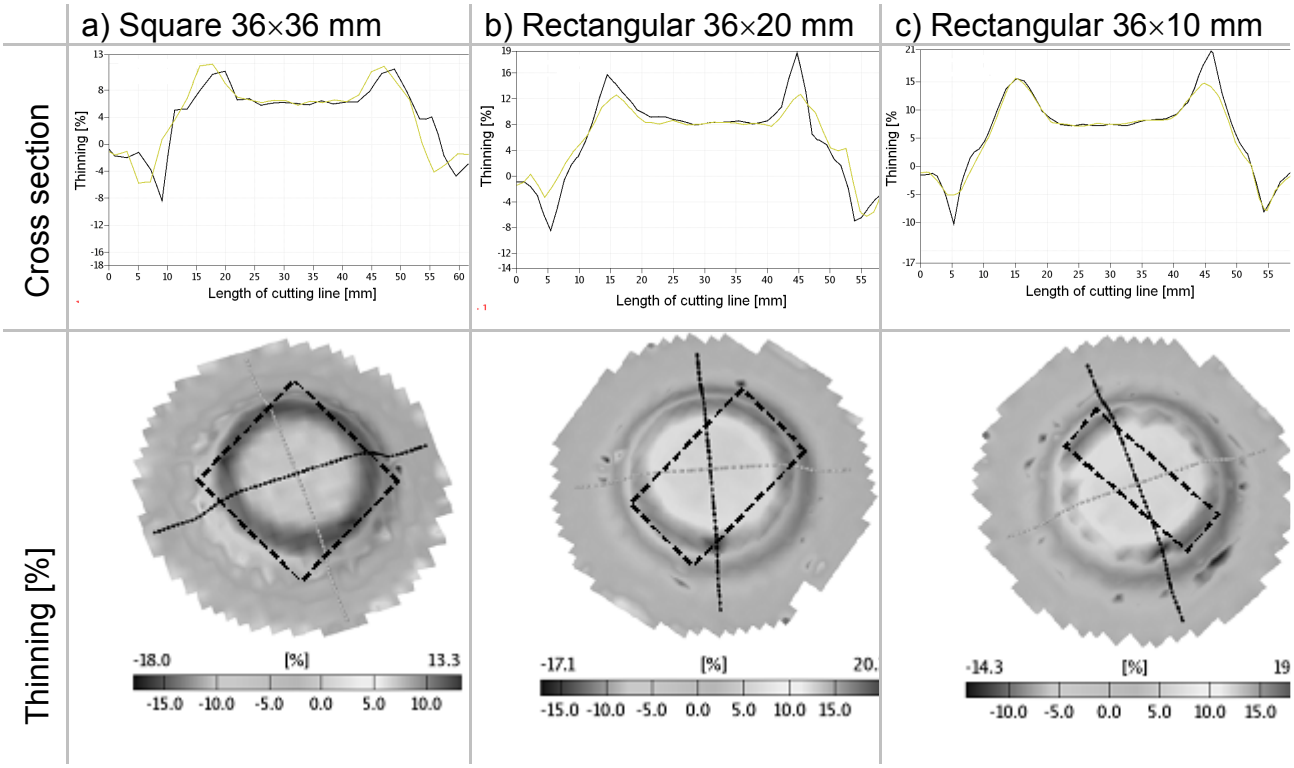

Fig. 30. Thickness reduction in SMS with different solid inlays. The positions of local inlays are marked

By analysing the forming behaviour of the sandwich's cover sheets, with and without circular reinforcement subsequent to the deep drawing test up to 10 mm via photogrammetry, the following results can be stated:

- Regions of high stress concentration are the blank holder area (see the principle strain diagram, Fig. 24) and the area of the circular blank (drawing process involves applying radial and tangential forces). In the case of sandwiches without reinforcement, the maximum of principle strain for this deformation is about 25 %, whereas using a circular solid steel inlay the principle strain value is reduced to 15%. Using a mesh steel reinforcement of the same diameter the thinning coefficient is about 21 %.
- The presence of local inlays stiffens and supports the total thickness.

During the deep drawing of reinforced sandwich structures with circular and rectangular inlay shapes, the size and the shape of the inlays play a significant role (Fig. 30). By centrally positioning the rectangular reinforcement to the flat drawing punch (Ø is 33 mm), initial cracks were observed in the transition region of "reinforcement-polymer" in the area "head-edge" of cup. In the case of circular reinforcement, here the forming process only involves metal materials (cover sheet/reinforcement/lower sheet). It was found for the deep drawing processes of sandwich samples with rectangular inlays, that by decreasing the reinforcement's size, there is an increase in cup height. Increased polymer area leads to the stress distribution over the transition region from the area of high loading ("head-edge" region) to the area with good drawing characteristics (edge or "flange region"). The thinning analysis of SMS, with their respective plate reinforcements, obtained by the photogrammetry subsequent to deep drawing tests to 10 mm is presented in Fig. 31.

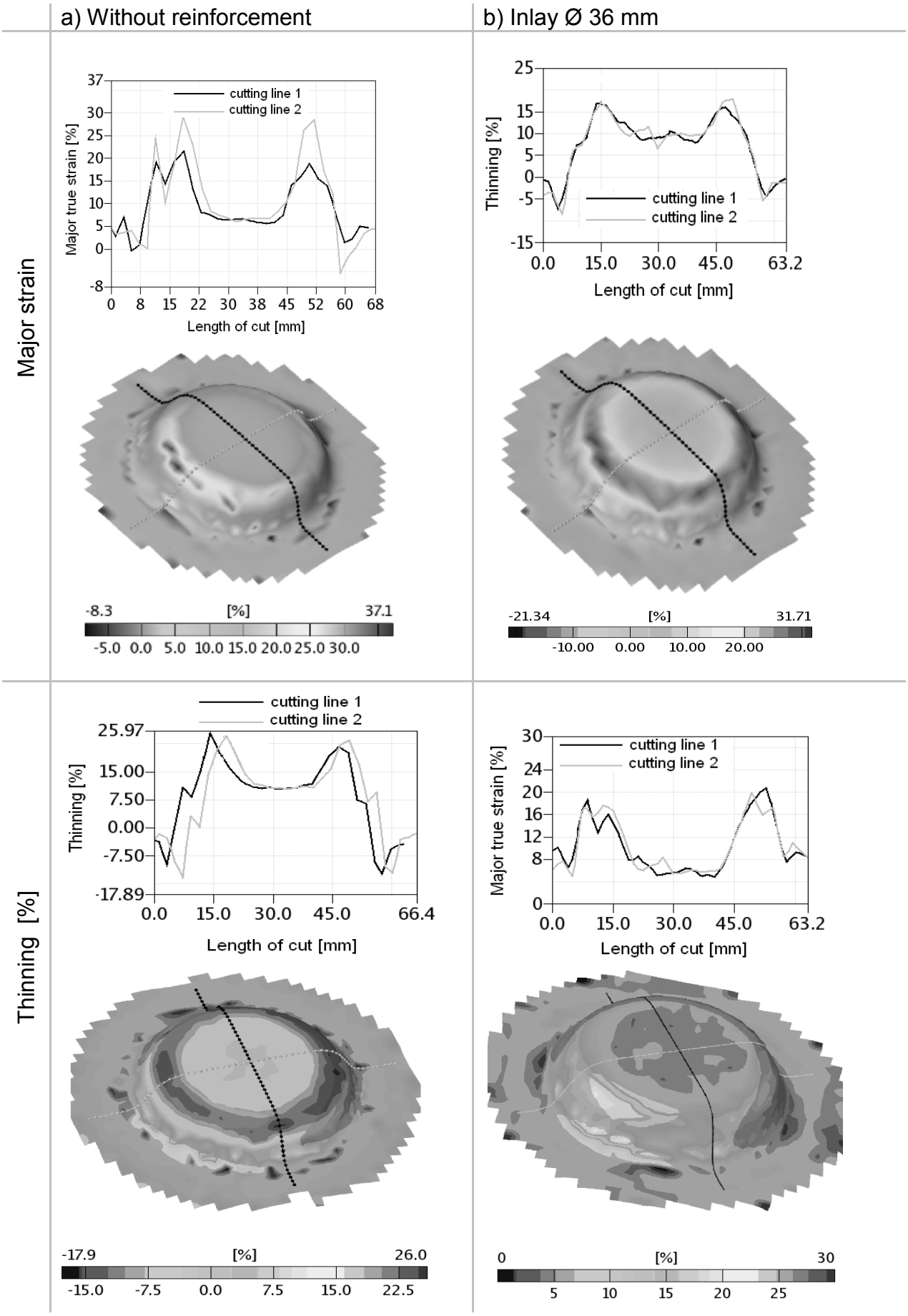

Fig. 31. Photogrammetry analysis of 316L/PP-PE/316L SMS (cover sheet) without (a) and with circle reinforcement (b) with Ø 36 mm inlay; deep drawing depth: h = 10 mm

As a result for these types and positioning of reinforcements is can be concluded:

- To improve the formability of reinforced sandwich composites the diameter of the inlay has to be higher (case of 40-60 mm of inlay) than the diameter of the punch (Ø 33 mm).
- Mash steel plates can be used instead of solid ones. Both variations exhibited good formability and a reduced thinning compared to the non-reinforced ones.
- A solution is given for special applications, e.g. the connection of parts with screws or in case of thermal joining focusing on the formability as well as weight reduction.

Deep drawing using standard geometries. This study was done to help to gain an understanding of each kind of reinforcement's influence on the drawing behaviour of off-centre inlays as well as the influence of the local inlays' geometry on the forming process of sandwich systems with extreme positions of the cup's transition region "head - wall".

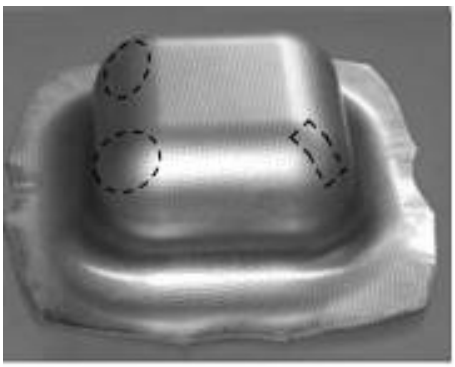

Fig. 32. Position of different reinforcement by the deep drawing with square punch 95×95 mm

In order to obtain the influence of different local reinforcement positions on the forming behaviour of SMS by deep drawing, the edge position of local inlays in the sandwich were selected as shown in Fig. 32. Large flat punches with circular, square and oval forms were chosen for the drawing punch's geometry. The local reinforcement was placed in the transition area "head - edge" of the cup to strengthen this region. As an example, a SMS sample is depicted in Fig. 32 where three local reinforcements in "edge - head" region of a square form are schematically presented. The dimensions of the SMS sheets used were 250×250 mm. .

The forming behaviours obtained from sandwich samples which were reinforced by three different reinforcements were investigated by means the deep drawing test using square devices at different degrees of deformation (up to 10, 20 and 30 mm).

For the reinforcements rectangular solid steel 36×10 mm and circular Ø 36 mm mashed and solid steel was chosen. The drawing parameters are given in Table 10.

Table 10. Testing parameters for deep drawing tests

		Deep drawing test
Blank holder pressure	[kN]	80.0
Speed of drawing	[mm/s]	0.6
Radius of punch angle	[mm]	25.0
Size of the punch	[mm]	95×95

As an example, the photogrammetric analysis of the sandwich sample, as shown in Fig. 32, is presented in Fig. 33. Deep drawing depth was 20 mm.

During the deep drawing process, cracks first appear in the corner without reinforcement. This can be explained by the strengthening of the other three corners and by the stress transition from the

edges with metal cores to the edge with the sensitive polymer core. The influence of each kind of reinforcement can be determined by the equal cap height of 20 mm resulting from the deep drawing test. In the non-reinforced region by photogrammetic analysis (right in front, Fig. 33), the maximum thinning value is $\varepsilon_{max} = 14.7$ %. The value of thinning for the rectangular reinforcement reaches a maximum of $\varepsilon_{max} = 11.4$ %. Sandwich samples with circular reinforcement exhibit thinning values of ε_{max} 10.6 % and $\varepsilon_{max} = 14.4$ % for solid steel and mesh inlays, respectively. Non-reinforced sandwich samples and those with mesh inlays exhibit a higher formability effect than the sandwich samples with solid plate inlays. Sandwich samples with rectangular reinforcement show a higher thinning effect. This may be due to the larger polymer area surrounding the local inlays compared to those ones with circular solid steel plates.

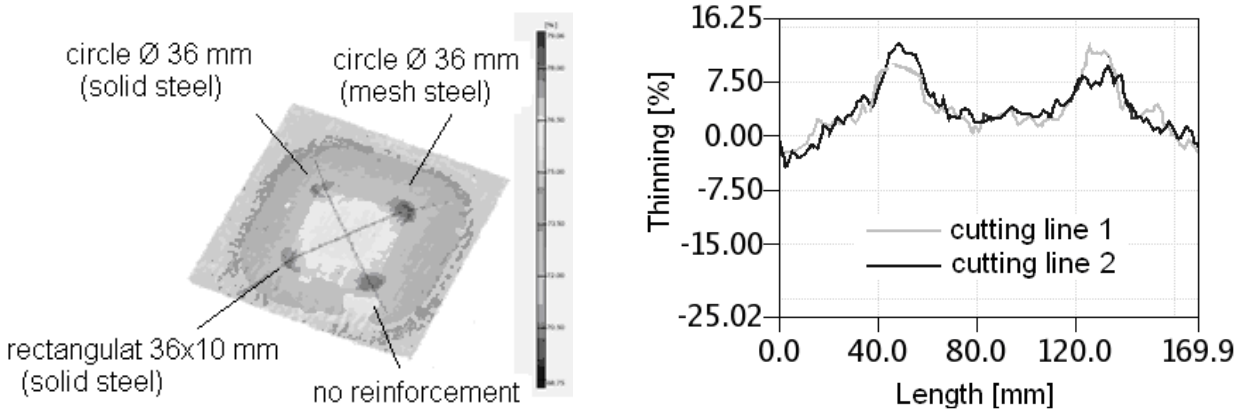

Fig. 33. Thinning of SMS with three different reinforcements: intersection 1 (grey) is the line between the rectangular 36×10 mm (solid steel) and circular Ø 36 mm (mashed steel), intersection 2 (black) the one between no reinforcement and circular Ø 36 mm (solid steel)

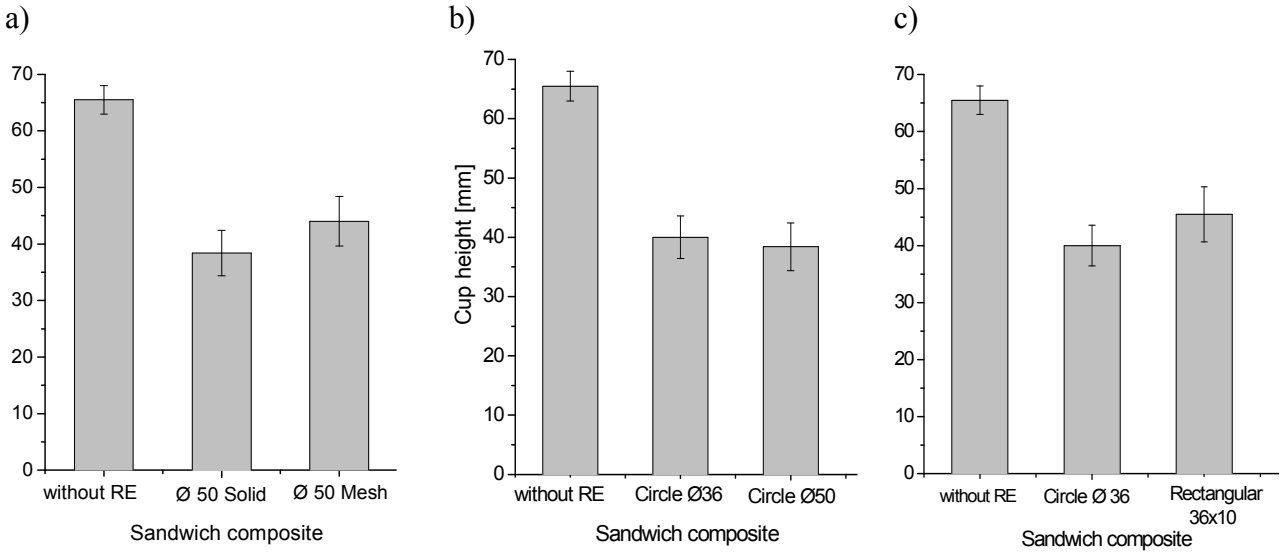

Fig. 34. Deep drawing test of SMS with and without reinforced elements: Influence of a) diameter of reinforcement, b) geometry of inlays and c) reinforcing material – solid steel sheet and steel mesh

In order to study the influence of each kind of reinforcement on the forming behaviour of SMS by deep drawing with the position of inlays at the square cup's corners, sandwich samples with one reinforcing element of each kind were produced and formed by deep drawing subject to the same conditions (see Table 10). The experimental results obtained by deep drawing of the sandwich samples with different inlays are presented in Fig. 34. Fig. 34 a-c show the influences of the size of the inlay's geometry and of the reinforcement's material on the forming behaviour by deep

drawing, respectively, where the reinforcing elements are positioned at the corners of the cup in the "head – wall" region.

The forming behaviours of SMS with off-centre inlay positions (head-wall area of the sandwich cup) are different. Fig. 34 a depicts the dependence of cup height on the reinforcement's diameter. It can be clearly seen that in general the maximum cup height is strongly reduced when a reinforcement is placed at the corners. With an increasing area of reinforcement in the corner region (e.g., the case of 50 mm of circle inlay), the cup's height decreases slightly.

On the other hand, with the circular Ø 36 mm (solid steel), the cup height is higher (≈ 40 mm) than that for the rectangular reinforcement (≈ 35 mm), (Fig. 34 b). In this case, the vertical position of the rectangular inlays to the forming direction is beneficial for the SMS's forming process. It can be clearly seen in Fig. 34 c that sandwich composites with mesh reinforcements show better formability compared to the sandwiches with solid plate inlays and coming closer to the non-reinforced results.

Bending tests

Forming by bending has been performed in order to investigate the flexural stress-strain response of the sandwich materials with and without local inlays. The technical implementation of the sandwich sheet bending involves numerous geometric and mechanical parameters which affect the technological process – diameter of punch tools, dimensions of bending equipment, adhesion between the sandwich layers as well as the post testing mechanical visco-elastic and failure behaviours of the sandwich materials subject to bending.

Due to the different geometry and number of loading rollers - punches using three-point (Fig. 32 a) and four-point (Fig. 32 b) bending processes - the behaviour of SMS with and without local reinforcements can be very different.

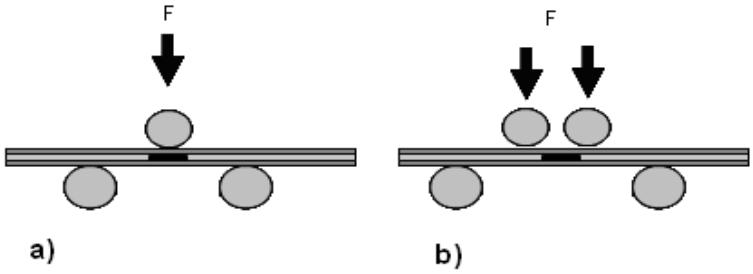

Fig. 35. Schematically exposition of three-point (a) and four-point bending (b) tests for SMS with local reinforcement (the position of local inlays is central)

The local reinforcement is initially placed at the centre of loading – directly under the punch (Fig. 35). By means of this extreme position of the local inlays directly under the bending rolls, the delamination behaviour of the sandwich laminates have been investigated using one or two rollers in the bending zone beneath the loading.

The viscoplastic behaviour of metal-polymer-metal samples (spring-back effect) as well as the delamination effects and failure of sandwich composite laminates with and without local inlays were determined and analysed following each kind of bending.

The influences of central positioning, geometry and of the local reinforcing material on the sandwich samples' bending process have also been studied by bending. Subsequent to flexural deformation, all sandwich samples were analysed with the aid of a photogrammetric analysis. The metal cover and lower sheets of sandwich laminates were raster-painted after the production process in order to analyse the thinning effect and to obtain the diagrams of maximum and minimum principle strains, and elongation by using DIC photogrammetry.

Three-point bending. Three-point bending tests were performed according to DIN EN 7438 [65]**.** Using the three-point bending method, the bending punch contacts the sandwich sample which is not fixed at its edges as shown in Fig. 36, where the geometrical dimensions of the equipment for the three-point bending are given, too.

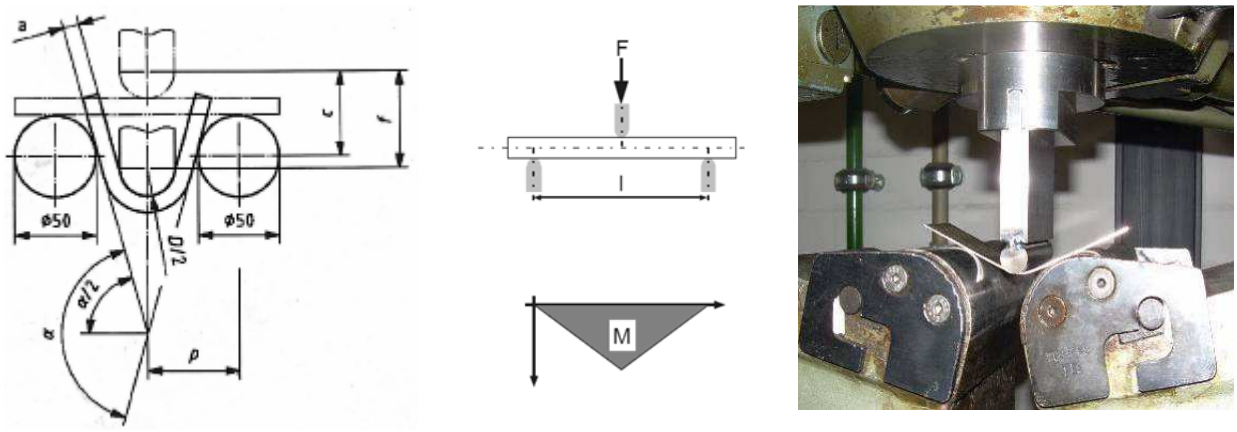

a) b) c)

Fig. 36. The dimensions of three-point bending (a), moments M by three-point bending (b), and photo of equipment (c)

The parameters of the three-point bending test for the 1.6 mm thick sandwich samples with size of 36×100 mm (Fig. 37a) are given in Table 11. A schematic diagram of the sandwich samples investigated on the three-point bending is depicted in Fig. 37.

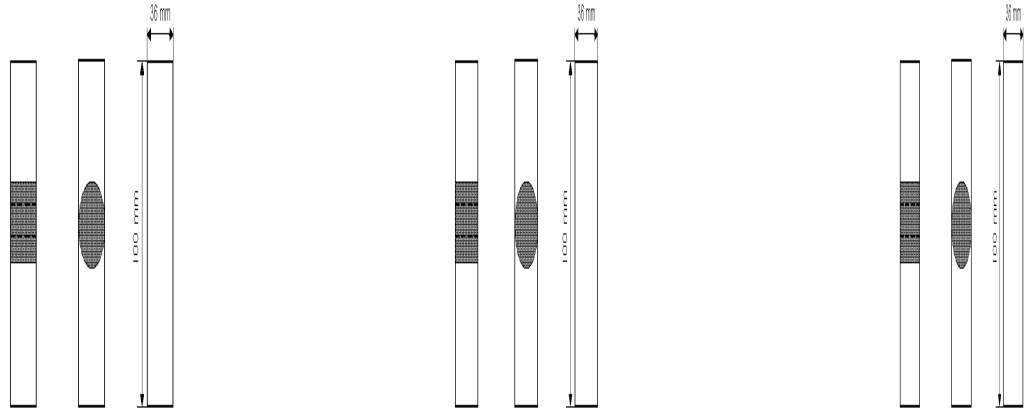

a) b) c)

Fig. 37. Sizes of three-point bending sandwich samples without reinforcement (a) and position of local reinforcement with square or rectangular shape (b) and circle inlays (c)

The bending angle α of the three-point bending sample was calculated for different bending depths following Eq. 6-8:

$$\sin\frac{\alpha}{2} = \frac{p \times c + W \times (f - c)}{p^2 + (f - c)^2} \tag{6}$$

where

$$W = \sqrt{p^2 + (f - c)^2 - c^2} \tag{7}$$

and

$$c = 25 + a + \frac{D}{2} \tag{8}$$

Table 11. Parameters of three-point bending tests

Parameter:		Size:
Sandwich thickness	a [mm]	1.6
Diameter of bending punch	D [mm]	6, 12, 24, 48
Diameter of lower rollers	d [mm]	50
Distance between the centres of lower fixed rollers	p [mm]	51.6+D
Distance in height of the punch from the starting to the finishing point	f [mm]	

The results of the bending tests with a 12 mm diameter punch are shown in Fig. 38 for SMS with and without different local reinforcements. The square 36×36 mm (Fig. 37 b), circular Ø 36 mm (Fig. 37 c) and rectangular 36×10 mm inlay shapes were selected for the local reinforcements. Sandwich samples were deformed up to their failure or delamination in order to investigate the failure mode as well as to determine the role played by the inlays' positional centrality (critical) on the sandwich laminates' forming behaviour during the bending process.

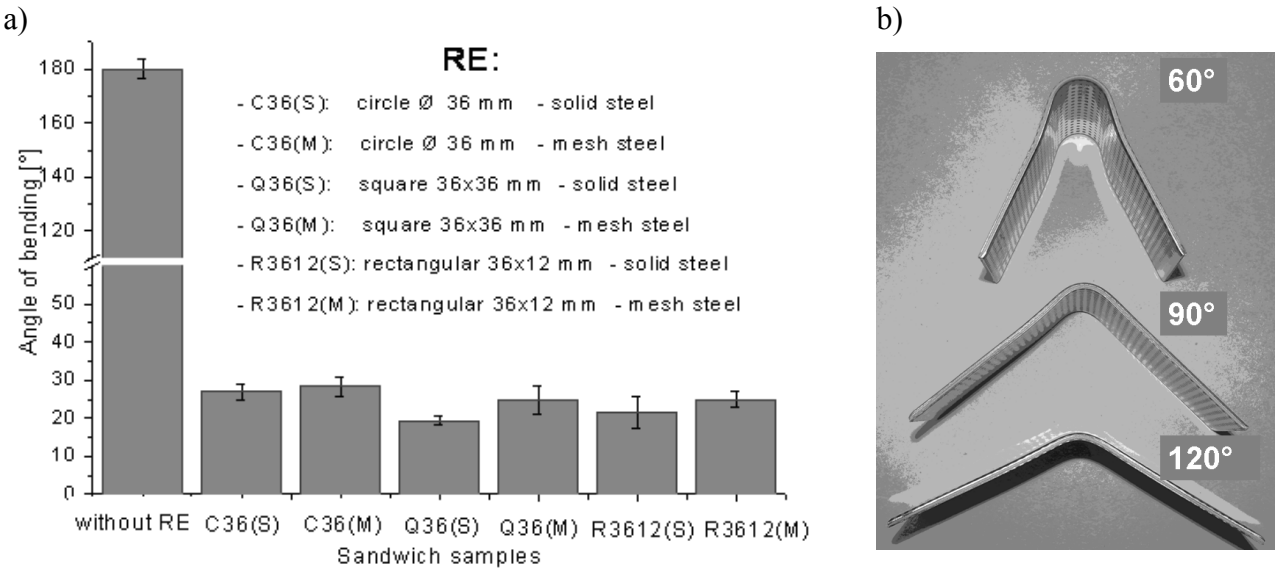

Fig. 38. Three-point bending test of SMS with a punch of Ø 12 mm and fixed rollers with Ø 50 mm. Distance between the centres of the rollers: p = 63.6 mm. Reinforcements: circular Ø 36 mm, square 36×36 mm and rectangular inlays with solid and mesh steel (a). Sandwich samples without reinforcement after three-point bending to 60, 90 and 180°

SMS samples without reinforcement clearly showed the expected behaviour due to the bending process: no delamination of the samples or micro cracking in the metal-polymer interface at the maximum possible bending angle (180°) could be detected.

In opposite to this for the sandwiches with local reinforcement, the reaction on forming is significantly different. The maximum bending angle (α_{max}) for reinforced sandwiches by circular, square and rectangular inlays was approximately 30° using a bending punch of Ø 12 mm. Within the different reinforcement types of sandwich samples there no large differences in the fracture strengths could be detected. The sandwich samples which are reinforced by steel mesh plates show slightly higher bending angles than those for sandwich samples with solid steel inlays. The reason will be the better bonding situation of the mesh types.

Sandwiches without reinforcement have good characteristics and can be bent up to the maximum bending angle (bending angle α_{max} = 180°). In contrast to this, sandwich laminates with centrally positioned local reinforcement exhibit less bending ability ($\alpha_{max} \approx 30°$). The failure of sandwich samples with local inlays is observed in the "inlay-polymer" region on both sides along the sandwich length. The reason for this premature failure of reinforced sandwich samples can be explained as following:

1) Using this combinations of sandwich and inlay geometry there is no sandwich area on the two opposite sides of the sample. Because of missing bonding or only very small areas being bonded, this leads to earlier cracks in the region of the reinforcement. The effect of increased bonding areas on the forming of SMS with local reinforcement in three-point bending will be described later.

2) The diameter of the punch (12 mm) is too small for this ratio of diameter to layer thicknesses: the size of reinforcement in the sandwich samples exceeds the punch diameter (e.g. by using of circular reinforcement with a diameter of 36 mm). For the three-point bending process, the maximum bending tension is concentrated in the region of the reinforcement at the punch area.

For increasing the bending abilities a bending punch with a larger diameter must be taken. Therewith one can avoid the regions of high bending stress concentration or reduce these concentrations to an acceptable level. Simultaneously the region of the local reinforcement's edges is exceeded. Another method to increase the bending forming potential for such reinforced sandwich systems is to apply cover sheets and fix the reinforcement between them

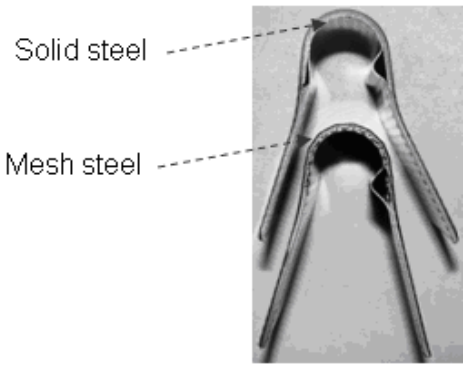

Fig. 39. Sandwich samples with steel mash and solid steel reinforcement with square geometry. Bending angle is 120°

In order to obtain more realistic forming behaviour of the reinforced sandwich samples, a fixture was designed, where sandwich samples were clamped between two supporting steel sheets with a thickness of 1 mm, each, by bolting them as shown in Fig. 40. The process of three-point bending was carried out then under the same conditions as mentioned before. The total thickness of the set was 3.6 mm.

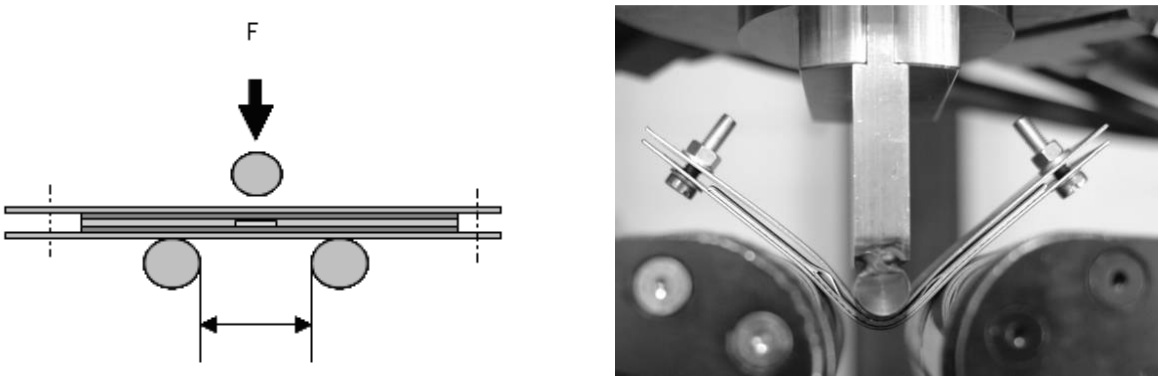

a) b)

Fig. 40. Support device for sandwich bending process: Sketch of supporting steel sheets 150 ×40×1 mm with clamped sandwich samples 100×36×1.6 mm (a) and a photo of the arrangement for three-point bending (b)

In order to further investigate the distribution of delamination in sandwich samples with local reinforcement, sandwich samples were deformed by three-point bending up to a bending angle of 180°. Fig. 39 shows sandwich samples with square inlays subsequent to bending up to 180°. The maximum bending angle for this type of sandwich without delamination is $\alpha_{max} \approx 30°$. The distribution of bending cracks was located at the transitional region of "RE-Polymer core".

The use of such a support enables sandwich samples with the mentioned different local inlays allows obtaining bending angles of $\alpha = 60°$ and 120° without failure or delamination of samples. The results of three-point bending tests for reinforced sandwich samples using circular and square reinforcements with and without the aid of the support device and a bending punch diameter of 48 mm are presented in [66] together with the formability analysis data.

In order to investigate the spring-back effect of sandwich samples with and without reinforcement, all samples were deformed by three-point bending and using the support device up to a bending angle of 60°. As an example the dependence of the reinforcement on the spring-back effect by bending to an angle of 60° is presented in Fig. 42. The spring back effect was calculated by using the equation:

$$\Delta\alpha=\alpha_{end}-\alpha_0 \tag{9}$$

where α_{end} is the angle after bending. α_0 represents the process bending angle (e.g. 60°).

Analysing the spring-back behaviour for three-point bending up to $\alpha_0 = 60°$, other modes of forming could be observed: Sandwich samples with circular reinforcements show a larger spring-back effect than both, sandwich composites without reinforcement and with mesh inlays. This phenomena is strongly dependent of type and size of the reinforcements, e.g. for sandwich laminates with circular reinforcement, a bending angle of 60° is insufficient to plastically deform the inlay due to its strength. So the spring-back effect reaches 14%. For the other combinations of inlays, the effect has a strongly reduced level of about 8-10%.

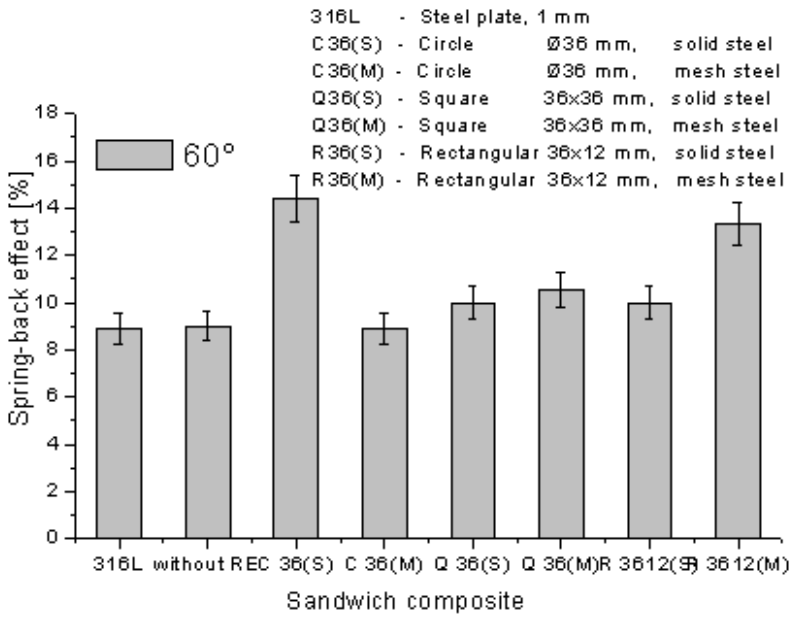

Fig. 41. Spring-back effect for a process bending angle $\alpha_0 = 60°$ and different types of reinforcements

Influence of the bending punch diameter on the forming behaviour for three-point bending. The maximal bending angle for sandwich samples with and without inlays can be increased by increasing the diameter of the bending punch. The dependency is presented in Fig. 40 a for SMS without local inlays and with circle reinforcements (Ø 36 mm, solid steel). Fig. 42 b shows bended samples, processed with different bending punch diameters.

It could be observed that sandwiches without reinforcement show an increase in the maximum bending angle from 114 up to 150° with increasing the bending punch diameter from 6 to 48 mm. For the small punch diameters, the bending stresses concentrate in a smaller region of the sandwich sample thereby leading to high bending tensions in the contacting area and resulting in early failure. On the other hand, the use of bending punches with larger diameters (e.g. 48 mm) results in a more homogeneous distribution of bending tension in the sandwich sample.

Using sandwich samples with circular reinforcements, a tendency for the three-point bending of SMS similar to SMS without RE could be observed: For bending punches with diameters of 6, 12 and 24 mm, the main concentration of bending tension becomes most severe for the sandwich with the 36 mm diameter reinforcement. For punch diameters larger than the inlay's dimensions, higher bending angles (90°) can be reached for the reinforced sandwich samples (Ø 46 mm bending punch and Ø 36 mm inlay).

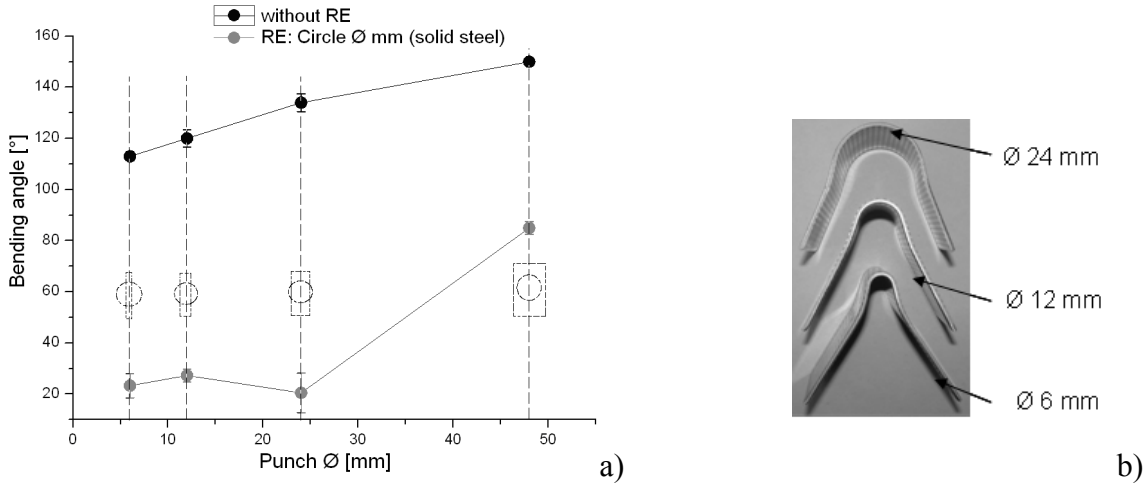

Fig. 42. a) Bending angle in dependency of the bending punch diameter for SMS without and with circle inlays (Ø 36mm, solid steel) (grey) for three-point bending,
b) sandwich samples without reinforcement after the bending test for different punch diameters. Dimensions of sandwich sample: 36×100 mm.

Three-point bending of sandwich plates with different local inlay positions to bending. The three-point bending tests were carried out on sandwich composites with circular and rectangular local inlays having different size and position to the bending load.

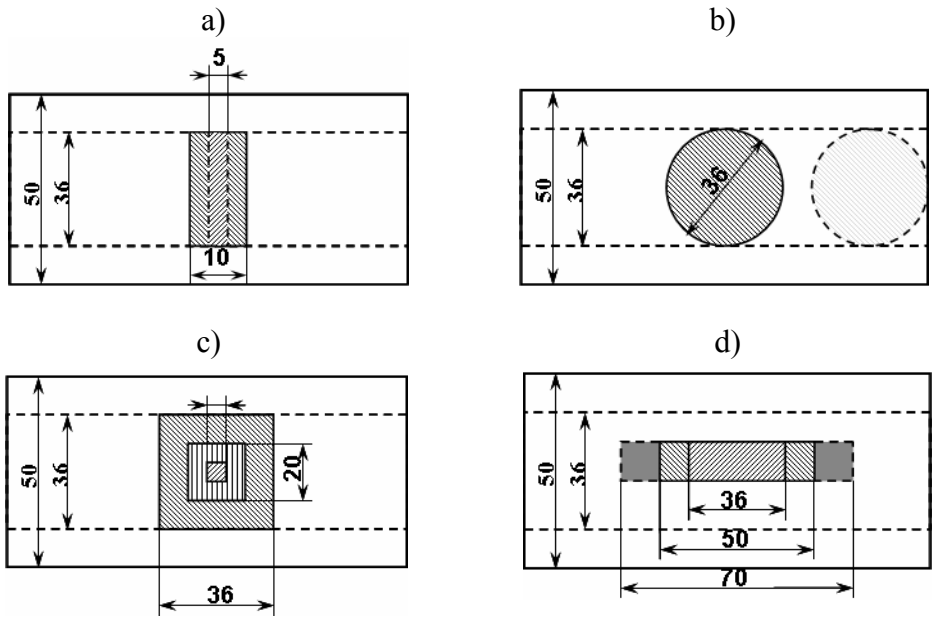

Fig. 43. Schematically exposition of sandwich samples for three-point bending process without support device. Local inlays are in central position. Sizes of rectangular inlays were 5×36, 10×36 (a); 30×10, 50×10, 70×10 mm (d), of square inlays: 36×36, 20×20, and 10×10 mm (c); diameter of circle reinforcement was Ø 36 mm.

In order to determine the role of polymer content and RE-shape on the formability of reinforced sandwich samples by three-point bending process, different sizes of rectangular and circular reinforcements were chosen, been positioned at the centre and the edge of the sample. The dimensions of sandwich samples were 36×100 and 50×100 mm, respectively. The investigations were carried out to ascertain the mechanical failure of such sandwich samples subject to bending loads. Fig. 43 schematically depicts sandwich samples with local inlays and the sandwich sample's size.

The three-point bending tests on reinforced sandwich samples were carried out by using the same parameters for the bending equipment, see Table 11. Sandwich samples were deformed up to failure (visible cracks or delamination of the sandwich samples). Fig. 44 shows the three-point bending test results for the above mentioned sandwich samples using the bending punch of Ø 12 mm. In Figs. 44 a-d the influence of the ration between sandwich width and dimension and type of reinforcement is presented. So, e.g. in Fig. 44 a "36×5(36)" describes a sandwich with a width of 36 mm and an inlay sized 36×5 mm. In Fig. 44 b the behaviour using different circle inlays were investigated, Fig. 44 c represents the results for a constant sandwich width and changing square sizes and Fig. 44 d, finally, gives the results for different positions and sizes of a 36 mm wide SMS sample.

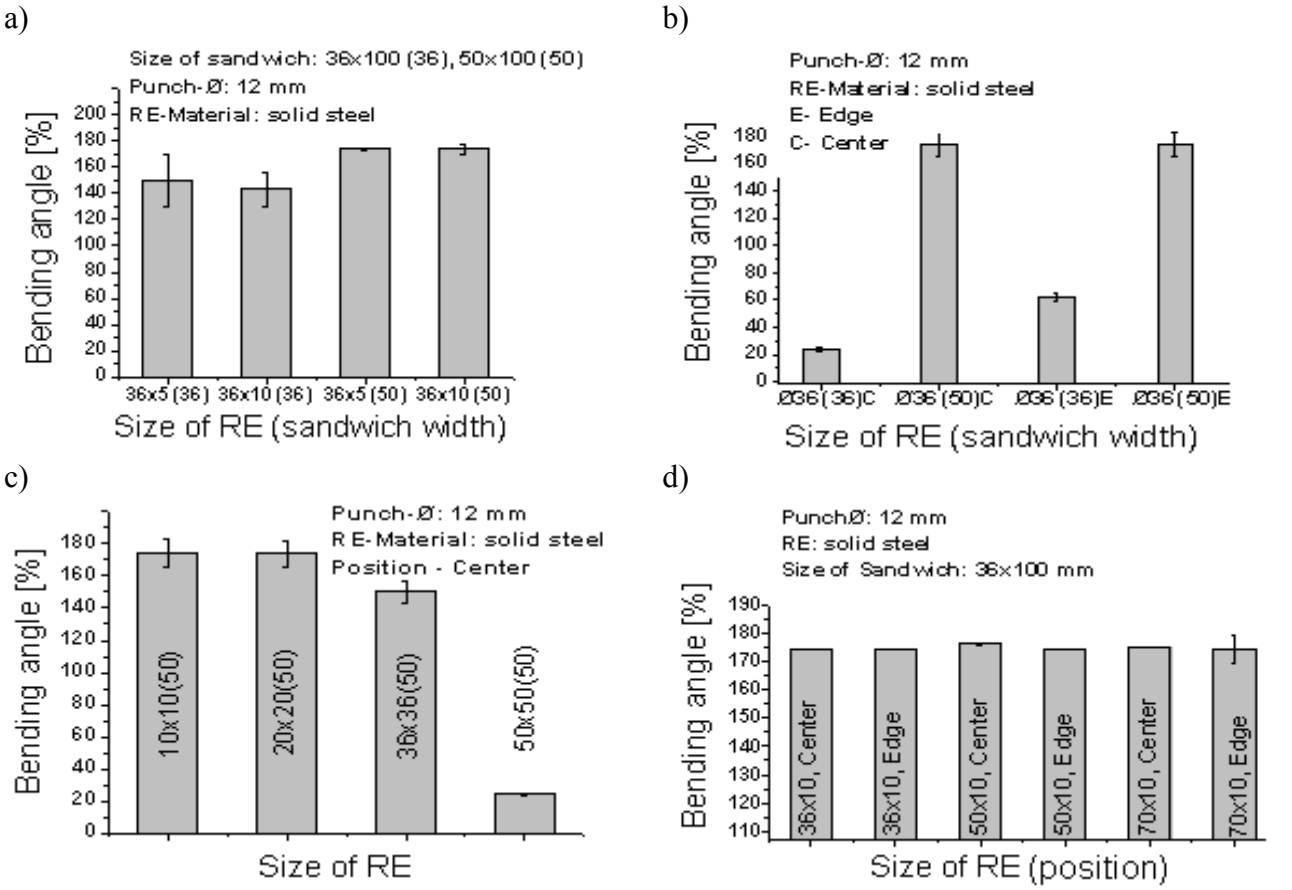

Fig. 44. Three-point bending test results for locally reinforced sandwich samples with centred and edge inlay positions.

It can be seen, that coming to a ratio close to 1 - that means for a reinforcement width close to the SMS width - the parts fail earlier. With a quite well bonding region around the inlay (case of 50×100 mm with inlay sizes less than 50 mm) the maximum bending angle is about 174° (see Fig. 44 c). Delamination can be observed at the transition region "RE-polymer foil" directly into the loading area.

Sandwich samples with the dimension of 36×100 mm for the sizes of RE: rectangular - 36×36, 36×10 mm and circle - 36 mm ^{Ø} as well as sandwich samples with the dimension of 50×100 mm and RE: 50×50 mm (that means close to ratio 1) show an earlier failure for centre positioned RE. Sandwich laminates with polymer regions around the rectangular local reinforcement (d) as well as those being placed at the edge of the SMS reach maximum bending angles (about 170°) without visible delamination or ultimate failure of the samples (Fig. 44 b and d).

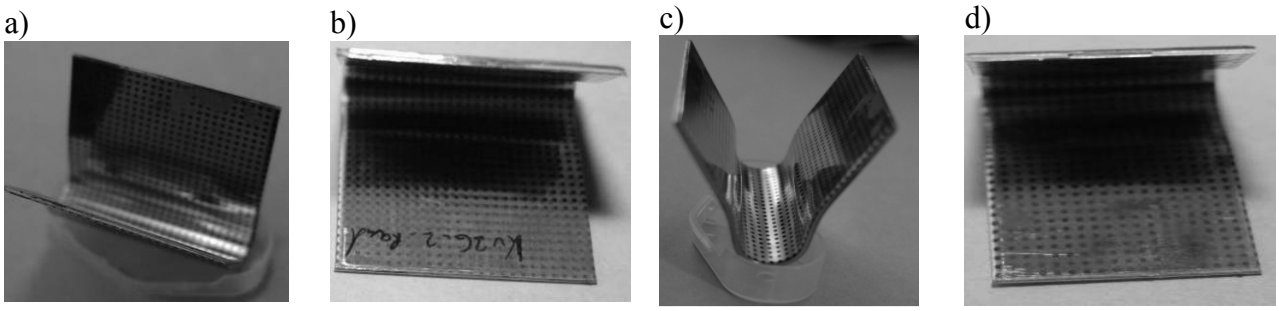

Fig. 45. SMS with circle solid steel inlays after the three-point bending tests. (a) central and (b) edge positions of RE.
Samples with rectangular solid steel inlays; (c) central and (d) edge positions of RE

It can be concluded that it is possible to subject reinforced sandwich samples to the three-point bending process without failure at high degrees of forming (bending angles 170-180°). The size of the inlays can be different; however, the local inlays should be surrounded by the core material, guaranteeing a good bonding contact to the cover sheets, or, for the edge case position, minimum from three sides with the core material. The maximum possible bending angle for sandwiches with circular and rectangular reinforcements, used, with central and edge positions was approximately 175-180°. The forming behaviour of reinforced sandwich composites can be related to the forming of sandwich samples without reinforcement.

Four-point bending test. The four point bending test was carried out using two loading rollers in order to investigate the forming behaviour of reinforced sandwich composites with centrally positioned local inlays. Here, the four-point bending process was based on the standard DIN EN 53293 [64] by using two movable rollers (punches) and two fixed punches (see Fig. 46 a). Fig. 46 b gives the development of the moment along the sample length. The geometrical data are listed in Table 12.

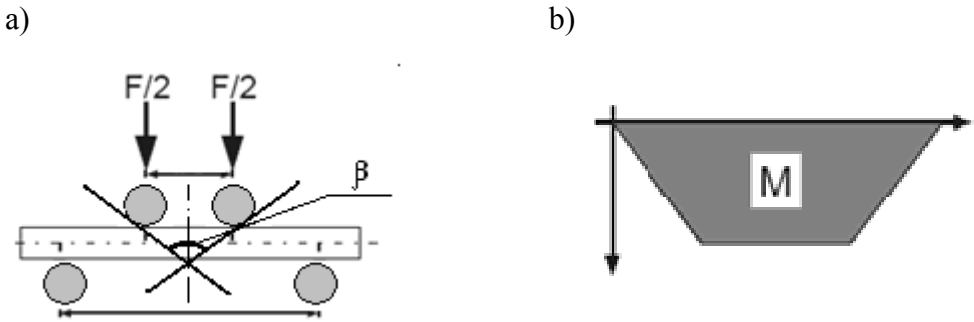

Fig. 46. Sketch of four point bending process: a) diagram of loading with the bending angle β, b) development of the moment

Table 12. Parameters of four-point bending tests

Parameter:		Size:
Sandwich size	[mm]	170x36x1.6
Diameter of bending punches	[mm]	12.0
Diameter of lower rollers	[mm]	50.0
Distance between the centres of lower punches	[mm]	147.6
Distance between the centres of upper punches	[mm]	99.2

The four-point bending process is more complex than the three-point bending process, producing a constant moment between the two punches. The bending load is realized by two movable points and the stress distribution is more uniform for four point bending.

In the four-point bending process, the diameter of movable punches is 12 mm and the diameter of the two fixed punches is 50 mm. The distance between the centres of movable punches is 99.2 mm. In order to investigate the spring-back effect and the failure behaviour of reinforced sandwich samples, the four-point bending was carried out up to 60°, 90° whereby the maximum bending angle for sandwich samples using the four-point bending process is β = 180°. Fig. 48 depicts the formability of sandwich samples with and without rectangular, circular and square solid steel reinforcements for these different bending angles.

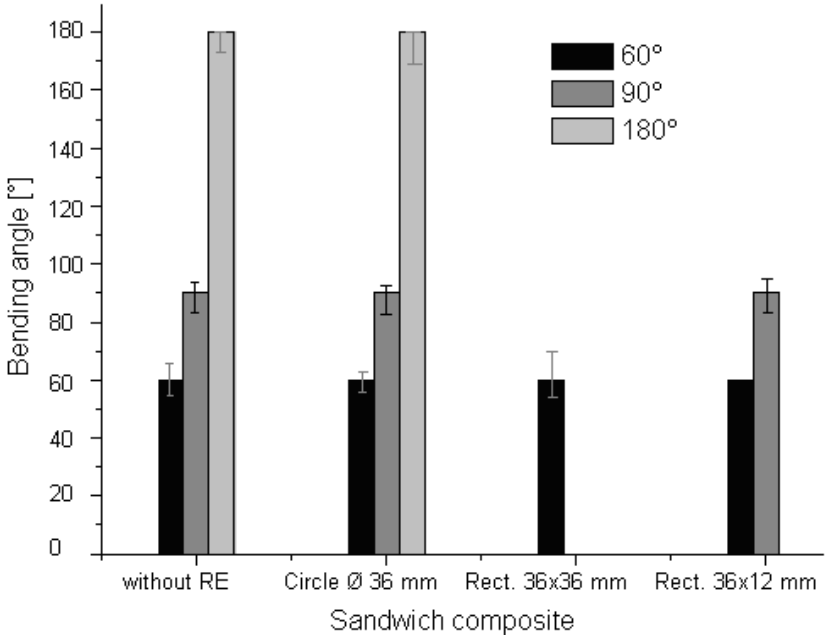

Fig. 47. Four-point bending of sandwich samples with and without RE of local solid steel circular Ø 36 mm, rectangular 36×12 mm and square 36×36 mm inlays

Sandwiches without reinforcement and with circular inlays reach the maximum bending angle β = 180° without visible delamination or failure. The maximum bending angle for sandwiches with the square reinforcements, used, is approximately β ≈ 60°. Sandwich samples with rectangular inlays reached the level of 90°. The reason of early failure of the sandwich samples with rectangular and square reinforcement is that – as described before - no sandwich area exists on two sides over width of the reinforcement, whereby in sandwiches with circular reinforcements, the inlay is surrounded by the polymer (compare three-point bending, Fig. 38 c). For these sandwich samples, the experimental results for the spring-back effect are presented in Fig 48 subsequent to four-point bending up to 60 and 90°.

In the four-point bending process for sandwiches with the centrally positioned inlays, the main bending tension is concentrated in the polymer regions on two sides of the inlays. It can be seen that the spring-back effect is higher for all sandwich composites subjected to a bending angle 60° than to a bending angle up to 90°. The bending angle of 60° is not sufficient to plastically deform the edges of sandwich samples. The values for the spring-back effect for all sandwich samples bent to 60° are quite similar. By bending to 90°, the edge regions of the sandwich samples can plastically deform, here the values of the spring-back effect are low and the difference in the values conforms to the difference in the plastic deformation in each sample.

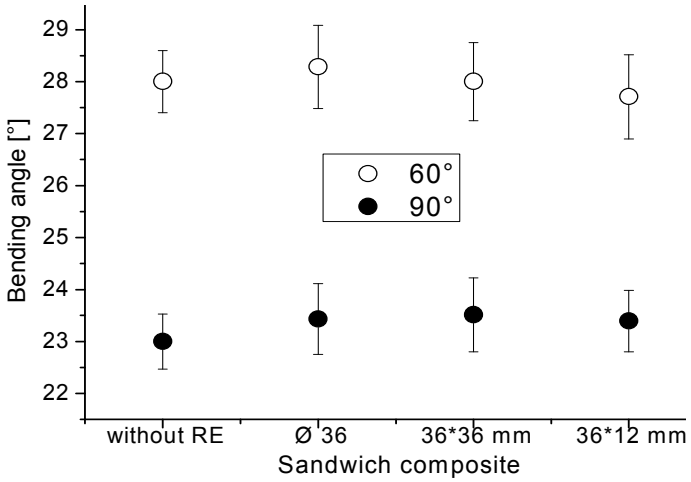

Fig. 48. Spring-back effect in four-point bending with bending angles of 60° and 90° for SMS with and without circular (Ø 36 mm), rectangular (36×12 mm) and square (36×36 mm) solid steel inlays

Three - roll bending process. The roll bending process was carried out in order to determine the mechanical behaviour and failure of 316L/PP-PE/316L SMS. Both, the elastic part (spring-back effect) as well as the failure (max angle of bending) of SMS was determined and analysed after the roll bending. The equipment used and the determination of the bending angles is presented schematically in Fig. 49.

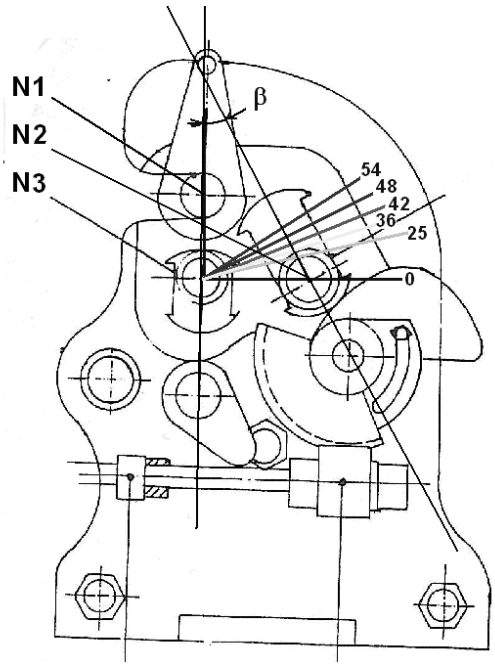

Fig. 49. Scheme of roll bending equipment with possible angles by roll bending. The diameter of each roll (N1-N3) is Ø 55 mm. Maximal possible bending angle is 54°. Angle between the axis of rolls is β = 35°.

The roll-bending tests were carried out according to DIN EN 7438 [68]. Sandwich samples were fixed between the two rolls (N1 and N3) and deformed by the third roll (N2) been moved 30° to the vertical axis. 25, 36, 42, 48 and 54° were chosen for bending angles.

As an example the experimental dependence of the spring-back effect on the roll-bending angles for sandwiches without RE and with local inlays (Ø 36 mm circular solid steel plate and rectangular reinforcement (36×10 mm solid steel sheet)) is presented in Fig. 50.

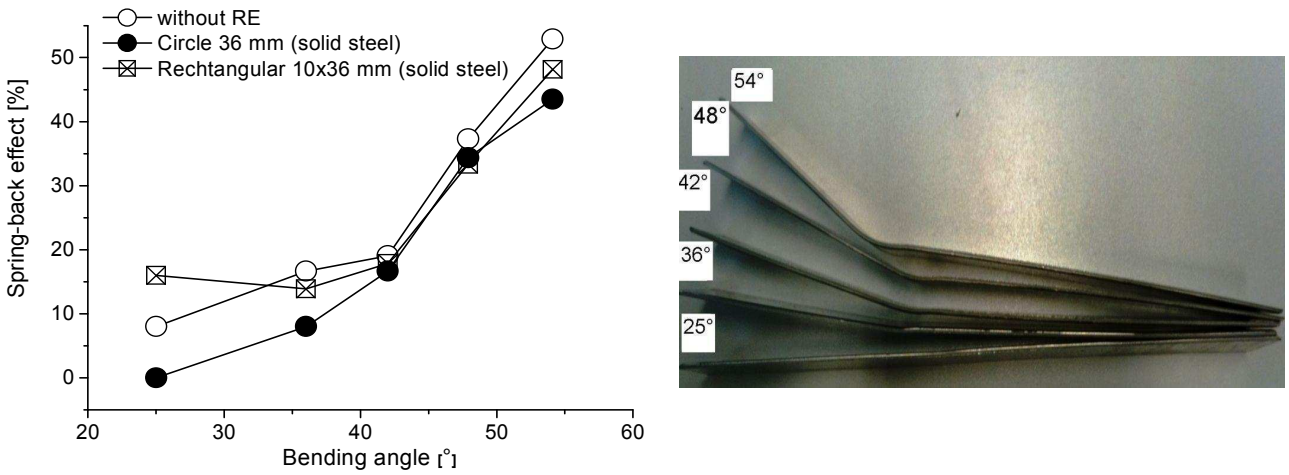

Fig. 50. Spring-back effect by roll-bending process for SMS without RE and reinforced by circle (solid steel Ø 36 mm) and rectangular (solid steel 36×36 mm) inlays (left). The picture of sandwich samples without reinforcement after roll-bending process until 25, 36, 42, 48 and 54° angles (right)

It can be seen that the spring-back effect increases strongly with the increase of the roll bending angle. The sandwich composite without reinforcement shows a slightly higher spring-back effect because of the existing elastic part (polymer core) without reinforcement in the sandwich sample. On increasing the bending angle in the sandwich core by roll bending up to 54°, the spring-back effect increases, too. Here, the circular reinforcement plays the role of locally strengthening the sandwich sample, by plastically deforming the region of the reinforcement.

Industrial applications of 316L/PP-PE/metal reinforced sandwich composite laminates. The experimental results for forming by drawing and bending, obtained for SMS with local reinforcement, demonstrate that the sandwich laminates exhibit a good potential for industrial applications as the are lightweight and good formable (by drawing and bending) materials. They can be mechanically and thermally joined using suitable reinforcements. Due to their good forming behaviour by deep drawing without large losses in plasticity in the strengthening region, SMS with solid steel and mesh steel plates can have applications in components for the automotive industry e.g. as a part of vehicle floor, which has to be welded and mechanical joined to the vehicle body (see Fig. 51).

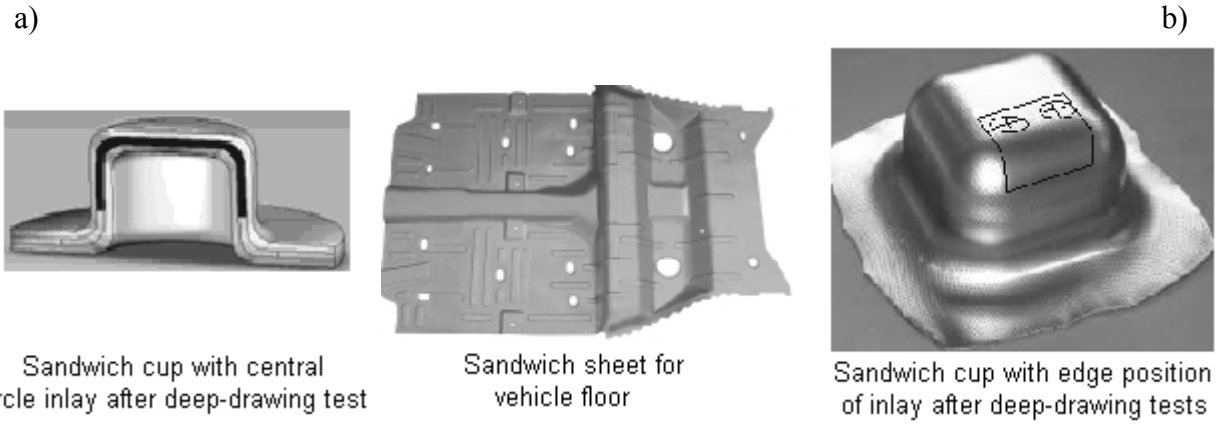

Fig. 51. CAD modelling of sandwich cup after deep drawing with local circle inlay in the area "head-edge" (a), vehicle floor part (b) and (c) deep drawn sandwich cup with schematically marked position of local reinforcement

Locally reinforced SMS can be used to strengthen cover sheets for vehicle roofs or doors in specific areas, due to the high forming and bending properties of SMS. These parts have to be thermally and mechanically joined to the vehicle's framework. Examples of mechanically and thermally joined regions at a door of a car are presented in Fig. 52.

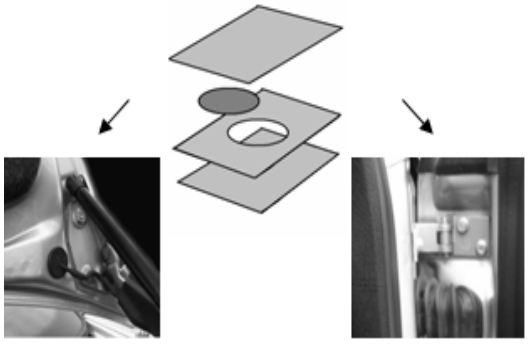

Fig. 52. Application of reinforced SMS like a cover sheets for auto roof plate with places of mechanical and thermal joining

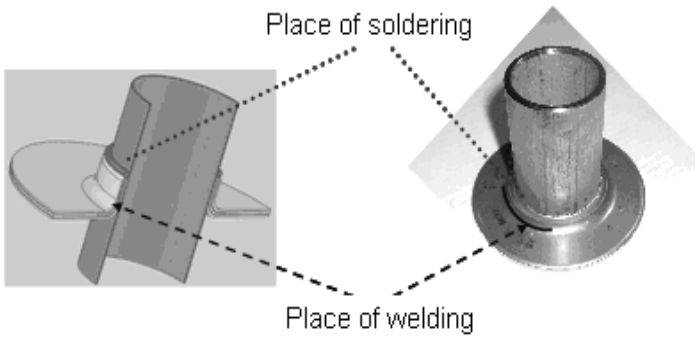

Fig. 53. Joint between a reinforced sandwich cup and a metal tube.
Possible places of RE for thermal joining; CAD draft (left), welded and soldered demonstator part (right)

For the thermal joining of hollow sections with sandwich panels reinforcements can support the joint in the area of joining strongly. In order to create complex sandwich constructions, the "sandwich plate or cup / metal tube" joining methods can be implemented. Due to the good formability of SMS with and without local reinforcements, sandwich cup – tube constructions, which are thermally joined by welding or soldering, become feasible, as can be seen in Fig. 53, where a sandwich with an inner hole, been reinforced with an inner metal ring of the same inner diameter, had been cantilevered. To create the edge area, the diameter of the drawing punch has to be larger than the diameter of the central holes. Thus, the punch diameter was chosen to 33 mm (diameter of drawing punch's envelop is 29 mm and radius of drawing punch at the edges is 1.5 mm) and the circular blank's diameter was 68 mm. The holes inside the sandwich samples had a diameter of 28.3 mm and 20.4 mm, respectively, so, with the chosen punch diameters a radius of 6.2 and 2.3 mm, respectively, had to be cantilevered. Some experimentally prepared sandwich cups with 50 mm circular reinforcements of solid steel following the deep drawing process to 10 mm and 5 mm are presented in Fig. 54.

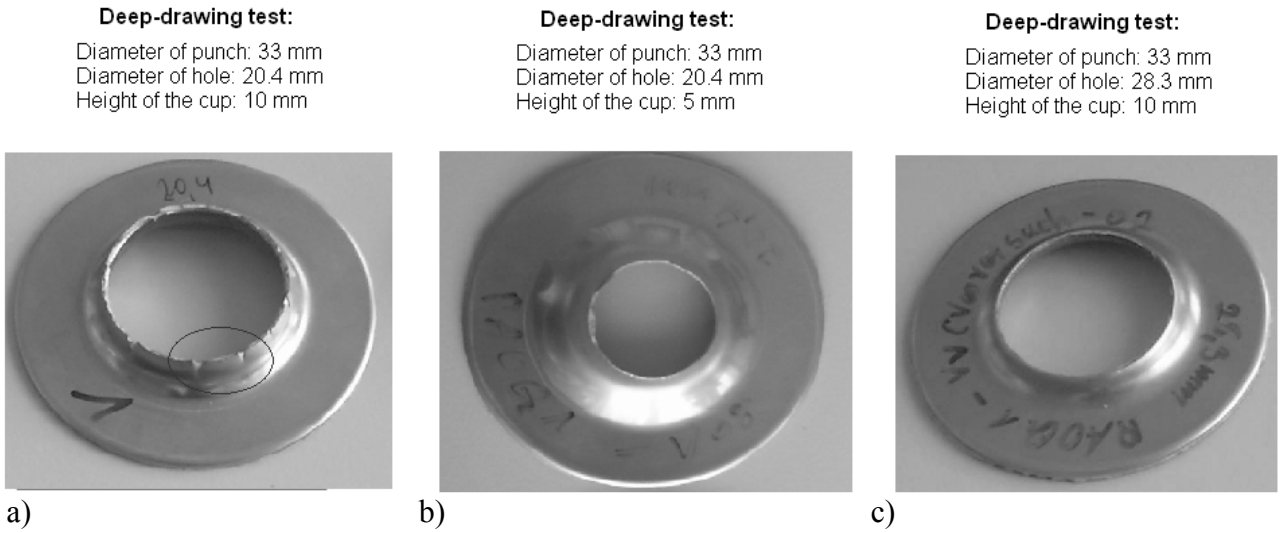

Fig. 54. Sandwich cups with local solid steel reinforcement (Ø 50 mm)

It is possible and suitable to produce cantilevered areas in adequately reinforced sandwich samples. The process is sensible to the ratio of punch to hole-diameter. When the diameter of the hole is too small, the high degree of deformation (bulging) leads to cracking and splitting, as can be seen in Fig. 54 a, b. On the other hand, the process of forming reinforced SMS is possible when the diameter of hole is slightly less than the diameter of punch (see Fig. 55 c). In order to produce the sandwich sample ready to be thermally joined with the metallic tube, whose external diameter is equal to drawing punch's diameter, the following conditions have to be fulfilled:

- The local square inlays have to be less than 80 % of the whole sandwich area in order to avoid the internal layers of SMS delaminating.
- The diameter of holes for the cup's flange area should be less than 10% of the punch's envelop.

Summary

In this paper the experimental and theoretical analysis and results of the forming behaviour of metal-polymer SMS is presented. The local plate inlays which

- provide the mechanical and thermal bonding of sandwich materials with other parts by the pressure loading due to their good strength properties ,
- provide for the design and adaptation of sandwich materials to the overall construction,

are continuing to attract special attention in current and future investigations.

The forming behaviour of metal-polymer-metal SMS with local plate and mesh reinforcement of different geometries and sizes, was measured and analysed by deep- and stretch drawing, three-point, four-point and roll bending processes. Stress-strain and thinning characterisation for the different degrees of the SMS's formability with local reinforcements were measured with the aid of photogrammetric analysis. All results were analysed using the metallographic characterisation of interfaces and bonding properties. The dependence of the sandwich materials' forming behaviour with and without local reinforcement was determined and analysed subject to the different forming conditions. The fields of application were pointed out corresponding to the obtained mechanical properties of reinforced sandwich structures.

Processing three-layer sandwich sheets by means of the roll bonding process has the capability to be used in continuous production. The local reinforcement of the sandwiches at special regions appears to be a solution for special applications, e.g. using screw fastening or thermal joining, with good formability obtained by deep drawing and, under special conditions, by bending processes.

Nevertheless the preparation technique for the production of reinforced sandwiches has to be developed. Deep drawing processes for complex structures using reinforcements have to be adapted, especially the understanding of the movement of local inlays during deep drawing and the dependencies from their shape.

Sandwich structures with a PP-PE foil core layer exhibit a great forming potential. The investigations up to now show that it is possible to reproducibly produce the sandwich material. In order to attain improved formability in reinforced sandwich laminates, the diameter of local circular inlays have to be larger than the punch diameter. To save weight in the construction, steel mesh plates can be used as reinforcing elements for industrial production. The sandwiches which have mesh reinforcement have better formability than those samples with solid steel plates.

The forming behaviour of locally reinforced located in the centre and edge positions in the sample reinforced sandwich composites in the three-point bending process, can be related to the forming behaviour of sandwich samples without reinforcement by using sandwich samples having large sandwich regions (metal-polymer-metal) surrounding three sides of the inlays.

Producing sandwiches with simple symmetrical rectangular inlay geometries which are centrally positioned to the drawing process is not beneficial for the deep drawing process. This is due to the presence of critical stress concentrations at the inlay's edges caused by drawing. The existence of vertical rectangular reinforcement at the edges of the cup's flange region (after the deep drawing process with a square punch) can be a good solution for locally strengthening these regions. It is possible to join "sandwich-cup / metal tube". Due to their forming properties, sandwich samples can be utilised as cover sheets for vehicle roof plates, strut mounting parts or other components in the automotive and shipbuilding industries.

For actually running investigations within the frame of this project questions will have to be answered concerning

- Optimisation of pre-treatment of surfaces
- Optimisation of inlay placing
- Influence of shape, type and position of the inlays in the sandwich sheet on the deep drawing conditions (movement of the inlays)
- Definition of border lines for the application of inlays (position and ratio of bonded / non-bonded areas)
- Tests under cyclic conditions.

References

[1] B. Harris, *A perspective view of composite materials development*, Materials & Design, 12, (1991) 5, pp. 259-272.

[2] J.L. Grenestedt, *New concepts for sandwich structures,* Sandwich Structures 7: Advancing with sandwich structures and materials; Proc. on the 7th int. conf. on sandwich structures, Aalborg, Danmark, 29-31 Aug. 2005, pp. 835–844.

[3] J.R. Vinson, *Sandwich Structures: Past, Present and Future*, Sandwich Structures 7: Advancing with sandwich structures and materials; Proc. on the 7th int. conf. on sandwich structures, Aalborg, Danmark, 29-31 Aug. 2005, pp. 3-12.

[4] D. Mohr, G. Straza, *Development of Formable All-Metal Sandwich Sheets for Automotive Applications*, Adv Eng Mat 7 (4) (2005), pp. 243–246.

[5] Th. Beumler, Fibre Metal Laminates – Application in the Aircraft Construction, Dresdener Leichtbausymposium (2001).

[6] L. Librescu, S-YOh, J. Hohe, *Dynamic response of anisotropic sandwich panels to underwater and in-air explosions*, Sandwich Structures 7: Advancing with sandwich structures and materials; Proc. on the 7th int. conf. on sandwich structures, Aalborg, Danmark, 29-31 Aug. 2005, pp. 97–106.

[7] L. Librescu, T. Hause, *Recent developments in the modelling and behaviour of advanced sandwich constructions: a survey*, Composite Structures, 48, (2000), pp. 1-17.

[8] Hrsg. ThyssenKrupp Stahl AG, Bondal® Körperschalldämpfender Verbundwerkstoff. 5/2003.

[9] W. Bisle, T. Meier, S. Mueller, S. Rueckert, *In-Service Inspection Concept for GLARE® –An Example for the Use of New UT Array Inspection Systems*, ECNDT 2006 - Tu.2.1.1. (2006), 19.

[10] M. von Tooren, *Airbus composite aircraft fuselages – next or never. Around glare: a new aircraft material in context*, Kluwer Acad. Publ. (2001), pp. 145-157.

[11] I. Burchitz, R. Boesenkool, S. van der Zwaag, M. Tassoul, *Highlights of designing with Hylite - a new material concept,* Materials science and Design 26 (2005), pp.271-279.

[12] A. Catella, *Support assembly for composite laminate materials during roll press processing,* USA patent publication. Pub. N: US 2006/0062950 A1. 2006.

[13] K. Behre, D. Klenke, S. Seidel, T. Walsch, *Verfahren zur Herstellung eines Verbundes,* Patentblatt 204/33. Int N: EP1445085A2, Alcan Technology and Management Ltd. (2004).

[14] A. Baldan, *Adhesively-bonded joints and repairs in metallic alloys, polymers and composite material*s, Adhesives, adhesion theories and surface pre-treatment, Journal of materials science 39 (2004), pp. 1-49.

[15] H. Palkowski, G. Lange, *Production of Tailored High Strength Hybrid Sandwich Structure*s, Materials Technology, steel research int. 79, No. 3 (2008), pp 27-36.

[16] G. Lange, A. Carradò and H. Palkowski, *Tailored Sandwich Structures in the focus of research Materials and Manufacturing Processes*, 24,10(2009), pp. 1150-1154

[17] A. Carradò, O. Sokolova, G. Ziegmann and H. Palkowski, *Press joining rolling process for hybrid systems*, Key Engineering Materials Vol. 425 (2010), pp 271-282.

[18] W. Michaeli, F. von Fragstein, K. Bahroun, *Oberflächen funktionalisieren,*. Kunststoffe 9/2009, pp. 64-68.

[19] D. Minzari, P. Møller, P. Kingshott, L.H. Christensen, R. Ambat, *Surface oxide formation during corona discharge treatment of AA 1050 aluminium surfaces,* Corrosion Science 50 (2008), pp. 1321–1330.

[20] I. Melamies, *Kaltes Plasma erobert neue Dimensionen,* Kunststoffe 9 (2009), pp. 56-61.

[21] J. Bishopp, *Surface pretreatment for structural bonding,* Handbook of Adhesives and Sealants-Basic Concepts and High Tech Bonding, Chapter 4, Volume 1 (2005), pp. 163-214.

[22] D.Zhang, G.Sun, L.C.Wadsworth, *Mechanism of corona treatment on polymer films*, Polymer engineering and science, June, Vol. 38, No 6, (1998), p. 965.

[23] S. Noeli, C.-J. Sinézio de C. *Surface composition analysis of PP films treated by corona discharge,* Mat. Res. 6, 2 (2003), pp. 163-166.

[24] M. Pascual, R. Balart L. Sanchez and other, *Study of the aging process of corona discharge plasma effects on low density polyethylene film surface*, Journal of Materials Science, 43, 14 (2008), pp. 4901-4909.

[25] P. Compston, W.J. Cantwell and others, *Comparison of surface strain for stamp formed aluminium and an aluminium-polypropylene laminate,* Journal of materials science 29 (2004), pp. 6087-6088.

[26] K.J. Kim, D. Kim, S.H. Choi and others, *Formability of AA5182/ polypropyleme/AA5182 sandwich sheets,* Journal of Materials Processing Technology 139 (2003), pp. 1-7.

[27] M. Weiss, B. Rolfe, M.E. Dingle and P. Hodgson, *The influence of interlayer thickness and properties on spring-back of SPS- (steel/polymer/steel) laminates,* Steel Grips, , 2, (2004), pp. 445-449.

[28] K.P. Jackson, J.M. Allwood, M. Landert, *Incremental forming of Sandwich panels*. Key engineering materials Vol. 344 (2007), pp. 591-598.

[29] M. Weiss, M.E. Dingle, F. P. Rolfe, D. Hodgson, *The Influence of Temperature on the Forming Behaviour of Metal/Polymer Laminates in Sheet Metal Forming,* Sandwich Materials Selection Charts Vol. 129, 2007, pp. 530-537.

[30] I. Burchitz, R. Boesenkool, S. van der Zwaag, M. Tassoul, *Highlights of designing with Hylite - a new material concept,* Materials science and Design 26 (2005), pp.271-279.

[31] W. Jung, W. Chu and S. Sahn, *Measurement and Compensation of Spring-back of a Hybrid Composite Beam*, Journal of composite materials, 41, 7(2007), p.851.

[32] M. Sadighi, H. Pouriayevali, M. Saadati, *Study of Indentation Energy in Three point Bending of Sandwich beams with Composite Laminated Faces and Foam Core,* World Academy of Science, Engineering and Technology 36, (2007), pp. 214-220.

[33] L. Lu, J. Wang, *Modelling of spring-back effect of metal-polymer-metal laminates,* Journal of Manufacturing Science and Engineering, 126(2004), p.599.

[34] Y. S. Chen, T.J. Hsu and S.I. Chen, *Vibration damping characteristics of laminated steel sheet,* Metallurgical and Materials Transactions A, 22, 3 (1991), pp. 653-656.

[35] W. Yong, C. Jun, T. Bing-tao, *Finite element analysis for delamination of laminated vibration damping steel sheet,* Trails. Nonferrous Mat. SOC. China 17(2007) 45, pp 5-360.

[36] C.M.C. Roque. O.T. Thomson, *Modelling of composite and sandwich plates by a trigonometric layerwise theory and multiquadrics.* Sandwich structures 7. Advancing with sandwich structures and materials, (2005), pp.231-240.

[37] S. Boria, G Forasassi, *Simulation of a crash-box for racing car based on sandwich material.* F2008-SC-016, 8th. World Congress on Computational Mechanics (WCCM8), 5th. European Congress on Computational Methods in Applied Sciences and Engineering (ECCOMAS 2008), June 30 – July 5, 2008, Venice, Italy.

[38] E. Doege, B.Behrens *Handbuch Umformtechnik, Grundlagen, Technologien, Maschinen* (2010) ISBN 978-3-642-04248-5.

[39] J. Feldhusen, S.K. Krishnamoorthy, *Fast joining and repearing of sandwich materials with detachable mechanical connection technology,* RWTH Aachen, Institute for Engineering Design (IKT)

[40] X. Sun, Ev. Stephensand, Dr. Herling, *Static and Fatigue Strength Evaluations for Bolted Composite/Steel Joints for Heavy Vehicle Chassis Components*, In 4th Annual SPE Automotive Composites Conference, Commercial Transport Session, Society of Plastics Engineers, Brookfield, CT. Paper No. 3, (2004), pp. 1-14.

[41] A. Kempf, *Entwicklung einer mechanischen Verbindungstechnik für Sandwichwerkstoffe*, Thesis, Dez. (2004).

[42] P. Bunyawanichakul, B. Castanie, J.-J. Barrau, *Experimental and Numerical Analysis of Inserts in Sandwich Structures*. Applied Composite Materials (2005), pp.177–191.

[43] O. Rabinovich, *Soft-core Sandwich Panels with Embedded Rigid Inclusions,* Journal of sandwich structures and materials, 9(2007), pp. 35-66.

[44] *Die NTD thermographische Systeme.* E/de/vis Betriebsanleitung. Edevis GmbH. (2008)

[45] Th. Zweschper1, G. Riegert1, A. Dillenz, G. Busse1, *Ultraschallangeregte Thermografie mittels frequenzmodulierter elastischer Wellen,* DGZfP-Berichtsband 86-CD, Thermografie-Kolloquium (2003), pp.45-52.

[46] T. Krell, J. Wolfrum, *Puls-Phasen-Thermographie an definiert geschädigten und reparierten Faserverbundbauteilen.* Wehrwissenschaftliches Institut für Werk-, Explosiv- und Betriebsstoffe – WIWEB, Thermografie-Kolloquium (2007).

[47] *Tantec elektrische Oberflächenbehandlung – Coronabehandlung* (Part 1), LabTEC Corona-Laborsystem (Part 2), Bedienungsanleitung Generator HV2010, HV2020, HV2002 (Part 3).

[48] H. Harwardt´s thesis, *Behandlung von PP- und PET-Substraten im Argon- und Methan/Argon-Plasma, 4*. Sept. (2006).

[49] Y. Tsai, L.C. Wadsworth, P.D. Spence, Pmc. 4th Annual TANDEC Conferen., Knoxville, Tenn. (Nov. 1994).

[50] A. Carradò, O. Sokolova, H. Palkowski, *Influence of corona treatment on adhesion and mechanical properties in metal-polymer-metal laminates systems*, Applied Surface Science (under review) March 13, 2010.

[51] DIN 53281 *Testing of adhesively bonded joints - Preparation of test specimens* 2006-06-00, p.14.

[52] DIN 53282, *Testing of adhesives for metals and adhesively bonded metal joints*; T-peel test, 1979-09-00, p. 2

[53] Th. Thales, D. Allen. *Lap shear and T-peel testing of seams in EPDM, CSPE and PVC for single-ply proofs,* International symposium on roofing Technology 1991, pp. 33-40.

[54] QVA-Z10-46-09, *Zweischnittiger Scherversuch an Verbindungselementen aus metallischen Werkstoffen*, Daimler Benz Aerospace Airbus, 2005-01.

[55] DIN 50114, Testing of metals; Tensile test on sheet or strip less than 3 mm thick, not using an extensometer. 1981-08-00.

[56] A. Carradò; J.Faerber; S.Niemeyer; G.Ziegmann; H. Palkowski, *Metal/polymer/metal hybrid systems: towards potential formability applications.* Composite Structures (under review: March 29, 2010).

[57] DIN 50101 (Ed: Deutscher Normenausschuss), Beuth Verlag GmbH, Berlin (1979).

[58] E. Doege, B. Behrens., *Handbuch Umformtechnik,* Grundlagen, Technologien, Maschinen (2007), p. 915

[59] H. Tschaetsch, Metal Forming Practise, Processes –Machines –Tools, ISBN-10 3-540-33216-2 © Springer-Verlag Berlin Heidelberg 2006.

[60] A. Godara, D. Raabe *Composite Science Technology* 67 (2007) p.2417–2427.

[61] *ARGUS v 5.4* Abridged User Manual.

[62] DIN 12004-2, Teil 2: Bestimmung von Grenzformänderungskurven im Labor (ISO 12004-2: 2008); Dt. Fassung EN ISO 12004-2:2008.

[63] *Aramis Benutzerinformation – Hardware.* GOM mbH, Braunschweig, (2007).

[64] *Aramis Benutzerhandbuch – Software. FLC Berechnung.* Hrsg. GOM mbH, Braunschweig, (2007).

[65] A. Carradò, O. Sokolova, H. Palkowski, *Formability of metal-polymer-metal sandwich composites with local metal reinforcements by using the deep drawing process,* Composite Structure (under review) May 11, 2010.

[66] H. Palkowski, G. Lange, *Production of Tailored High Strength Hybrid Sandwich Structures*, Materials Technology, steel research int. 79, No. 3 (2008), pp 27-36.

[67] DIN 53293. *Prüfung von Klebungen – Biegeversuch.* DK 62-416: 620.174.

[68] DIN EN ISO 7438, 2000-07 *Metallische Werkstoffe – Biegeversuch* (ISO 74: 2005); Deutsche Fassung EN ISO 7438, Beuth Verlag GmbH, Berlin (2005).